Modulation of C5a–C5aR1 signaling alters the dynamics of AD progression

Klebea Carvalho[1†], Nicole D. Schartz[2†], Gabriela Balderrama-Gutierrez[1], Heidi Y. Liang[1], Shu-Hui Chu[2], Purnika Selvan[2], Angela Gomez-Arboledas[2], Tiffany J. Petrisko[2], Maria I. Fonseca[2], Ali Mortazavi[1] and Andrea J. Tenner[2,3,4*]

Abstract

Background: The complement system is part of the innate immune system that clears pathogens and cellular debris. In the healthy brain, complement influences neurodevelopment and neurogenesis, synaptic pruning, clearance of neuronal blebs, recruitment of phagocytes, and protects from pathogens. However, excessive downstream complement activation that leads to generation of C5a, and C5a engagement with its receptor C5aR1, instigates a feed-forward loop of inflammation, injury, and neuronal death, making C5aR1 a potential therapeutic target for neuroinflammatory disorders. C5aR1 ablation in the Arctic (Arc) model of Alzheimer's disease protects against cognitive decline and neuronal injury without altering amyloid plaque accumulation.

Methods: To elucidate the effects of C5a–C5aR1 signaling on AD pathology, we crossed Arc mice with a C5a-overexpressing mouse (ArcC5a+) and tested hippocampal memory. RNA-seq was performed on hippocampus and cortex from Arc, ArcC5aR1KO, and ArcC5a+ mice at 2.7–10 months and age-matched controls to assess mechanisms involved in each system. Immunohistochemistry was used to probe for protein markers of microglia and astrocytes activation states.

Results: ArcC5a+ mice had accelerated cognitive decline compared to Arc. Deletion of C5ar1 delayed or prevented the expression of some, but not all, AD-associated genes in the hippocampus and a subset of pan-reactive and A1 reactive astrocyte genes, indicating a separation between genes induced by amyloid plaques alone and those influenced by C5a–C5aR1 signaling. Biological processes associated with AD and AD mouse models, including inflammatory signaling, microglial cell activation, and astrocyte migration, were delayed in the ArcC5aR1KO hippocampus. Interestingly, C5a overexpression also delayed the increase of some AD-, complement-, and astrocyte-associated genes, suggesting the possible involvement of neuroprotective C5aR2. However, these pathways were enhanced in older ArcC5a+ mice compared to Arc. Immunohistochemistry confirmed that C5a–C5aR1 modulation in Arc mice delayed the increase in CD11c-positive microglia, while not affecting other pan-reactive microglial or astrocyte markers.

Conclusion: C5a–C5aR1 signaling in AD largely exerts its effects by enhancing microglial activation pathways that accelerate disease progression. While C5a may have neuroprotective effects via C5aR2, engagement of C5a with

†Klebea Carvalho and Nicole D. Schartz are co-first authors

*Correspondence: atenner@uci.edu

[2] Department of Molecular Biology & Biochemistry, University of California, Irvine, 3205 McGaugh Hall, Irvine, CA 92697-3900, USA
Full list of author information is available at the end of the article

Carvalho *et al. Journal of Neuroinflammation*   (2022) 19:178

Page 2 of 21

C5aR1 is detrimental in AD models. These data support specific pharmacological inhibition of C5aR1 as a potential therapeutic strategy to treat AD.

Keywords: Complement, Inflammation, Alzheimer's disease, C5aR1, C5a, Disease-associated microglia, Mouse model, Therapeutic target

Background

Alzheimer's disease (AD) is the most common form of dementia and is characterized by the accumulation of extracellular amyloid beta (Aβ) plaques, hyperphosphorylated tau, synaptic loss, neuronal death, and ultimately cognitive decline [1]. Evidence suggests that inflammatory pathways are induced by amyloid and tangle accumulation, contributing to AD pathologies, and exacerbating neuronal injury and cognitive decline [2–4].

The complement system is a powerful effector of the innate immune system that is activated via three distinct pathways, classical, lectin, and alternative, all of which converge on proteolytic cleavage of C3 into the chemoattractant C3a and opsonin C3b. C3b also forms part of the C5 convertase, which cleaves C5 into C5a, a potent pro-inflammatory chemoattractant, and C5b, the initiating molecule of the lytic membrane attack complex (MAC) [5]. C1q, the recognition molecule of the classical pathway, in complex with the proteases C1r/C1s enables synaptic pruning as well as complement activation by fibrillar amyloid, which in the presence of C4, C2, C3, and C5 lead to the generation of C3a and C5a, both of which induce potent pro-inflammatory responses via their respective receptors C3aR and C5aR1 [6]. In addition, administration of C5a to neurons in vitro is neurotoxic and enhances neurodegeneration [7, 8].

In two mouse models of AD, pharmacologic inhibition of the C5a receptor (C5aR1) with PMX205 reduced amyloid plaque accumulation, attenuated activation of microglia and astrocytes, and protected mice against hippocampal synaptic loss and cognitive decline [9]. Inhibition or ablation of C5a–C5aR1 activity has also been demonstrated to increase survival and lower motor deficits in models of amyotrophic lateral sclerosis (ALS) [10, 11], reduce seizure susceptibility and inflammation in experimental epilepsy [12, 13], and accelerate functional recovery after spinal cord injury [14]. These data are consistent with detrimental consequences of C5a–C5aR1 activity in neurodegenerative diseases, including AD, and that inhibition of C5a–C5aR1 signaling may slow or prevent the progression of these diseases. Importantly, C5aR1 antagonists have been shown to be nontoxic in human clinical trials and case studies [15–17]. Genetic ablation of C5aR1 attenuated spatial memory decline and rescued neuronal integrity in the hippocampus in the Arctic mouse model of AD. This was accompanied by decreased inflammatory gene expression and enhanced expression of genes associated with debris clearance and phagocytosis in microglia, all supporting protective effects specific to C5aR1 inhibition [18]. However, the molecular and cellular pathways involved remain to be discerned. Recent studies suggest that microglial activation can influence the reactive states of astrocytes [19]. Whether C5aR1 ablation and the subsequent reduced microglia-mediated inflammation influences astrocytes in AD models remains to be determined.

C5aR1 expression is highly induced in AD mouse models [20]. To further elucidate the role of C5a–C5aR1 signaling in amyloid-associated cognitive decline, and to expand on our previous behavioral studies examining the role of C5a–C5aR1 signaling on cognitive decline in the Arctic mouse, we crossed the Arctic mouse to a model that overexpresses C5a under the control of the glial fibrillary acidic protein (GFAP) promoter and tested spatial memory with the object location memory (OLM) test [18, 21]. The dynamic transcriptomic and immunohistochemical changes due to C5a overexpression or C5aR1 ablation in Arctic mice were assessed using 6 mouse genotypes at 2.7, 5, 7, and 10 months of age. Since astrocytic and other cell-specific genes were missing from the analyses in our previous study, here, we microdissected the hippocampus and cortex of mice at different ages for bulk RNA-sequencing to identify region-, age-, and amyloid-specific transcriptomic changes. We identified more abundant changes in expression in hippocampi compared to cortices, correlating with higher amyloid pathology localization. We detected either decreased or delayed expression of AD-, disease-associated microglia (DAM), and reactive astrocyte-associated genes upon C5aR1 knockout. C5aR1 ablation also led to delayed expression of genes enriched for inflammation, microglial activation, phagocytosis, and cholesterol biosynthesis. Furthermore, we observed accelerated cognitive decline in the ArcC5a+, consistent with the hypothesis that C5a–C5aR1 signaling is deleterious in combination with amyloid pathology. Interestingly, C5a overexpression induced genes associated with synapse assembly, transcription, and GABAergic synapses, and may suggest parallel stimulation of C5aR1 and alternative receptors, as a result of the high transgene-driven expression of C5a, thus emphasizing the importance of specific targeted inhibition of C5aR1.

Carvalho *et al. Journal of Neuroinflammation*   (2022) 19:178

Page 3 of 21

Methods

Animals

The Institutional Animal Care and Use Committee of University of California at Irvine approved all animal procedures, and experiments were performed according to the NIH Guide for the Care and Use of laboratory animals. Mice were grouped housed in ambient temperature and given access to food and water ad libitum. The Arctic48 mouse model of AD (hereafter referred to as Arc), which carries the human APP transgene with three mutations—the Indiana (V717F), the Swedish (K670 N+M671 L), and the Arctic (E22G), was generated on a C57BL6/J background and originally provided by Dr. Lennart Mucke (Gladstone Institute, San Francisco, CA). This hemizygous mouse model produces fibrillar plaques as early as 2 to 4 months of age [22]. C5a-overexpressing mice, created by cloning the coding region for the C5a fragment of C5 plus a signal sequence into a construct containing the GFAP promoter to induce production and secretion of C5a as a function of GFAP induction [23], were crossed to Arc+/− mice generating wild type (WT), Arc, C5a+ and ArcC5a+ mice. C5aR1KO mice, created by targeted deletion of the C5a receptor 1 gene [24] (originally provided by Dr. Rick Wetsel, Univ. of Texas Health Science Center, Houston), were crossed to Arc+/− mice to generate mice homozygous for C5aR1 deletion with and without the Arctic transgene. These mice were used to assess the effect of C5a overexpression on amyloid-associated cognitive decline, as well as the effects of C5a overexpression or C5aR1 ablation on microglial-, astrocytic-, and AD-associated gene expression and microglial and astrocytic pathology in WT and Arc mice from 2.7 to 10 months of age. Both male and female mice were used in all experiments.

Behavior

Object location memory (OLM) as previously described [18, 21] took place in dim lighting in testing arenas (37.3 × 30.8 × 21.6 cm) covered with approximately 1 cm of sawdust bedding. Briefly, mice were handled for 2 min each per day over 5 days in the testing room and were acclimated to the testing arena for 5 min per day over 6 days. The first day of habituation was used as an open field test to measure locomotion and anxiety-like behaviors. During the familiarization trial, two identical objects (e.g., 100 mL glass beakers, blue Duplo Legos, or opaque light bulbs) were placed in opposite and symmetrical locations in the testing arena and mice were allowed to freely explore the objects for 10 min. After a 24-h delay, mice were tested for object location memory. One object was moved to the opposite end of the arena and exploration of both objects was tracked for 2 min. The object moved to a novel location was counterbalanced

to control for side preference. To prevent olfactory distractions, objects were cleaned with 10% ethanol and bedding was stirred after each trial (different bedding was used for males and females). Trials were recorded by mounted cameras from above and object exploration was scored manually by two blinded experimenters using stopwatches. Discrimination indices were calculated with the formula: [(time spent with moved object − time spent with unmoved object)/time spent with both objects) × 100] to obtain a percent (%) discrimination index (DI) [21]. Mice were removed from the analysis if they spent less than 1 s/min with the objects during training and/or testing or if the performance of mice was ±2 standard deviations from the mean.

Immunohistochemistry (IHC)

Mice were deeply anesthetized with isoflurane and perfused transcardially with cold phosphate buffered saline (PBS; 137 mM NaCl, 2.7 mM KCl, 4.3 mM Na_2HPO_4, 1.47 mM KH_2PO_4, pH 7.4). Half brains were quickly dissected and fixed in 4% paraformaldehyde for 24 h, then stored in PBS with 0.02% sodium azide at 4 °C. 30–40 μm coronal sections were generated using a vibratome and stored in PBS with 0.02% sodium azide at 4 °C until ready for use.

Sections were incubated in blocking solution (2% BSA plus 5% normal goat serum or 10% normal goat serum, and 0.1% Triton X in PBS) for 1 h on a shaker at RT. Tissues were then incubated with primary antibody diluted in blocking solution overnight on a shaker at 4 °C. Primary antibodies used were rabbit anti-Iba1 (1:1000, Wako #019-19741), rat anti-CD68 (1:700, Biolegend #137001), rat anti-CD11b (1:100, Biorad #MCA74G), hamster anti-CD11c (1:400, Biorad #MCA1369), rat anti-Lamp1 (1:500, Abcam #ab25245), rat anti-mouse C3 (1:50, Hycult #HM1045), rabbit anti-GFAP (1:2900, Dako #Z0334). Alexa Fluor secondary antibodies were diluted 1:500 in blocking solution and included 568 goat anti-Armenian hamster (Abcam, #ab175716), 555 goat anti-rat (Invitrogen #A21434), 488 goat anti-rat (Invitrogen #A21212), 488 goat anti-rabbit (Invitrogen #A-11070), and 647 goat anti-rabbit (Invitrogen #A21244). To counterstain fibrillar plaques with Thioflavin-S (Thio-S) sections were incubated in 0.1% or 0.5% Thio-S for 10 min after secondary antibody. To counterstain fibrillar plaques with Amylo-Glo (1:100 in PBS, Biosensis #TR-300-AG), tissues were incubated for 10 min before the first blocking step, washed in PBS for 5 min, and quickly rinsed with MilliQ H_2O before continuing with the IHC protocol. Sections were mounted and coverslipped with Vectashield (VECTOR). Low magnification images (10×) were acquired using ZEISS Axio Scan.Z1 Digital Slide Scanner. The mean areas of C3, GFAP, CD11b,

Carvalho *et al. Journal of Neuroinflammation*   (2022) 19:178

Page 4 of 21

CD11c, CD68, Iba1, and plaques were quantified in the hippocampal regions CA1, CA3, and DG, as well as the entire hippocampus and cortex using the Surfaces feature of Imaris ×64 (version 9.5.0). Confocal images were acquired at 20× using a Leica SP8 confocal microscope. Z stacks of 1-μm-step interval within a depth of 30 μm were obtained per area of interest, and volume was analyzed with Imaris. Quantitative comparisons between groups were carried out on comparable sections of each animal processed at the same time with same batches of solutions, unless otherwise noted.

Enzyme-linked immunosorbent assay
To confirm that mice expressing the C5aGFAP+/− transgene produce higher quantities of C5a protein, we performed enzyme-linked immunosorbent assay (ELISA) on pulverized hippocampus and cortex and on plasma taken from WT, Arc, C5a+, and ArcC5a+ mice at 5, 7, and 10 months. Pulverized cortex and hippocampal samples were homogenized on ice using a pestle pellet motor in 10× volume of homogenization buffer containing PhosphoSTOP (Roche) and cOmplete Mini Protease Inhibitor Cocktail (Roche) in TPER. Samples were then centrifuged at 14,000 rpm for 30 min at 4 °C and supernatant was collected and stored at − 80 °C. C5a concentration was determined with the R&D Systems Mouse Complement Component C5a DuoSet ELISA (DY2150) according to the manufacturer's instructions, in triplicate. Optical density was read on SpectraMax Plus 384 using and SoftMax Pro 7.1 (Molecular Devices, San Jose, CA). Standard curve was fitted to 4-parameter logistic expression. The total protein concentration was assessed using the Pierce BCA Protein Assay Kit (Thermo Scientific). Any plates lacking a full standard curve were normalized to the previous plate while C5a levels were averaged to generate one value per animal for samples repeated in more than one ELISA experiment. To assess whether the C5aGFAP transgene resulted in peripheral effects, plasma levels of C5a were measured. Blood collected via cardiac puncture was mixed immediately with 10 mM EDTA on ice. After centrifugation (5000 rpm for 10 min, 4 °C), plasma was collected and diluted 1:80 in reagent diluent for ELISA. When plasma from FVB/NJ C5-deficient mice [25] was assayed no C5a was detected, validating our C5a ELISA.

RNA extraction
Mice were perfused with PBS and dissected cortex and hippocampus were stored at − 80 °C prior to RNA extraction. Hippocampus and cortex were lysed separately in RLT (Qiagen # 80204) buffer with 1% β-mercaptoethanol by the QIAGEN TissueLyser. Total RNA of each tissue was extracted using the QIAGEN RNeasy mini kit and QIAcube (Qiagen # 80204 and # 9002864) and quantified using the NanoDrop ND-1000 spectrophotometer. The RNA integrity number (RIN) was assessed using the Agilent 2100 Bioanalyzer and the samples with RIN > 8.0 were used for library preparation.

RNA-seq library preparation
Bulk sequencing experiments were conducted utilizing 5–10 mice per genotype per age (with approximately equal numbers of males and females). RNA-seq libraries were built following the Smart-seq2 protocol using the Nextera library preparation kit [26]. In brief, polyadenylated RNA was reverse transcribed and a template-switching oligo (TSO) was added, which carries 2 riboguanosines and a modified guanine to induce a locked nucleic acid (LNA). cDNA was then amplified, and the resulting fragments were tagmented. Fragments between 150 and 600 nucleotides were finally selected using Ampure XP beads. The quality of all libraries was assessed using the Agilent 2100 Bioanalyzer. Bulk libraries were sequenced using the NextSeq 500 (Illumina) obtaining at least 10 million reads per RNA-seq sample. Resulting Fastq files and data matrices were deposited in GEO with the Accession ID: GSE197591.

RNA-seq processing and data analysis
Paired-end RNA-seq reads were aligned to mm10 reference genome and annotated with Gencode v21 transcriptome using STAR v.5.1 [27]. Gene expression was calculated using RSEM v1.2.25 [28]. Possible noise introduced by batch effects was corrected by the R (version 3.6.2) package Combat-seq [29]. Data were then normalized using edgeR trimmed mean of *M*-values (TMM) function [30]. TPM was calculated utilizing a custom script and ComBat-seq batch corrected counts as input. Two statistical outliers were removed based on dimensionality reduction by PCA and Pearson correlation coefficient [31]. A total of 372 RNA-seq data sets were generated. We also provide an explorable data viewer that presents all generated RNA-seq data (http://crick. bio.uci.edu:3838/ArcticMonday/).

Differential expression analysis
The R package maSigPro (version 1.58.0) was used to identify gene expression changes over time allowing for *k*-means clustering of genes that present similar patterns of expression during the time-course [32]. In addition, edgeR (version 3.28.1) was used to identify genes differentially expressed between selected ages and genotypes [30] using a false discovery rate (FDR) of 1% and an alpha of 0.05. We utilized expression as TMM-normalized counts represented as a count per million (CPM) matrix in both aforementioned packages.

Carvalho *et al. Journal of Neuroinflammation*   (2022) 19:178

Page 5 of 21

Gene ontology and pathway analysis

Gene ontology enrichment analysis was performed using Metascape and DAVID online tools computing gene-set overlaps between pathways and biological processes, that were selected based on *p*-values smaller than 0.05 [33, 34].

Statistical analyses

Unless otherwise stated, all statistical analyses were performed with GraphPad Prism (V9.3.1). When appropriate, comparisons were performed with two-way ANOVA and Tukey's post hoc test.
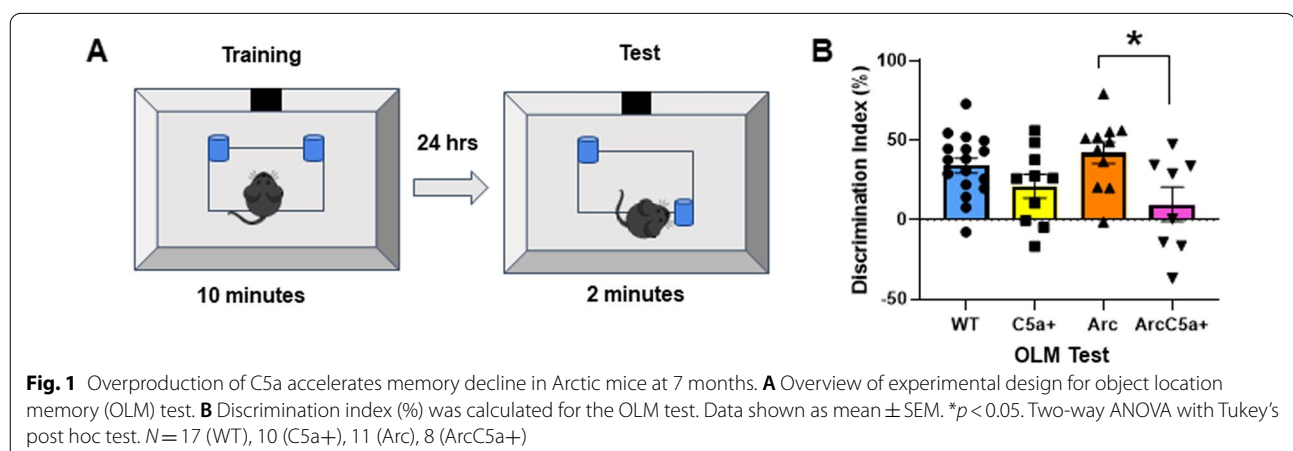
Results

C5a–C5aR1 signaling accelerates hippocampal-dependent memory deficits in Arctic mice

We previously reported that ablation of C5aR1 in Arc mice prevents memory deficits assessed with the OLM test at 10 months of age [18], suggesting that binding of C5a to C5aR1 induces responses that contribute to the cognitive decline observed in this model. Since elevated C5a production could result in greater engagement of C5a with C5aR1, we assessed whether transgene-driven generation of the C5a fragment accelerates the effects of this receptor signaling. We first confirmed that the C5a+transgene resulted in elevated levels of C5a in the cortex and hippocampus in both WT and Arctic mice without increasing plasma levels (Additional file 1: Fig S1), as expected since it is under the control of the GFAP promoter. Arc and ArcC5a+ mice and their WT littermate controls were tested at 7 months to determine if overexpression of C5a in brain would accelerate memory decline in the presence or absence of amyloid pathology. Analysis of open field revealed that there were no abnormalities in locomotion or anxiety-like behavior (Additional file 1: Fig S2A–C). All mice had similar total exploration times of both objects (Additional file 1: Fig S2D) and none showed a preference for either object position during OLM training (Additional file 1: Fig S2E). At 7 months of age, Arc mice did not show a deficit in object location memory compared to WT (Fig. 1). However, while no deficit was detected in the C5a-overexpressing wild type, the DI of ArcC5a+ mice was 6.2%, indicating significantly diminished cognitive performance compared to Arc mice (41.9%) (Fig. 1B). These data suggest that higher levels of C5a act in collaboration with co-existing amyloid pathology (which also results in induced expression of C5aR1) to accelerate cognitive decline. Taken together, and with the data published in 2017 [18], these findings are consistent with the hypothesis that chronic stimulation of the C5a–C5aR1 accelerates memory decline in Arc mice, whereas ablation of C5aR1 protects against it.

Neuronal loss and cognitive decline are common features of Alzheimer's disease [1]. Therefore, to determine if hippocampal-dependent cognitive decline in Arc and ArcC5a+ mice paralleled neuronal injury in the hippocampus, we assessed levels of dystrophic neurites (Lamp1) (Additional file 1: Fig S3A–B, E). While ArcC5aR1KO mice had lower levels of Lamp1-positive dystrophic neurites compared to Arc in the CA1, CA3, and DG of the hippocampus and in the cortex at 5 months (and in the DG at 7 months) (Additional file 1: Fig S3E) by 10 months the levels of LAMP1 were comparable in Arc and ArcC5aR1KO. ArcC5a+ had similar levels of Lamp1 as Arc, with a reduction only in the DG at 7 months (Additional file 1: Fig S3E). To determine if the toxic response to fibrillar plaques was altered with the deletion of C5aR1 or overexpression of C5a, we compared the relative levels of Lamp1 to Amyloglo (AG) levels in Arc, ArcC5aRKO, and ArcC5a+ (Additional file 1: Fig S3C, D, F, G). While there were minimal reductions of

Fig. 1 Overproduction of C5a accelerates memory decline in Arctic mice at 7 months. **A** Overview of experimental design for object location memory (OLM) test. **B** Discrimination index (%) was calculated for the OLM test. Data shown as mean ± SEM. *$p < 0.05$. Two-way ANOVA with Tukey's post hoc test. *N* = 17 (WT), 10 (C5a+), 11 (Arc), 8 (ArcC5a+)

Carvalho *et al. Journal of Neuroinflammation*   (2022) 19:178

Page 6 of 21

AG at 7 months in the ArcC5aR1KO CA3 and DG hippocampal regions (Additional file 1: Fig S3F), the ratio of Lamp1 to AG was significantly reduced in ArcC5aR1KO and ArcC5a+ at 10 months (Additional file 1: Fig S2G). These data suggest that while there may not be lasting changes in fibrillar plaque accumulation in ArcC5aR1KO or ArcC5a+ mice, the toxic response to these plaques is reduced.

Distinct subsets of genes are affected by C5ar1 knockout or C5a overexpression

To explore molecular basis of C5a–C5aR1 signaling, we dissected 372 cortices and hippocampi of mice representing six distinct genotypes (WT, C5aR1KO, C5a+, Arc, ArcC5aR1KO, and ArcC5a+) throughout disease progression at 2.7, 5, 7, and 10 months of age in order to build RNA-seq libraries and thus identify transcriptome changes in different cohorts (Fig. 2A). UMAP dimensionality reduction showed clear tissue-specific clustering characterized by the separation of cortices from hippocampi samples on UMAP 1. UMAP 2 showed a subtle separation of tissues from younger mice located at the top and tissues of older mice located towards the bottom of the axis in hippocampus samples, and left to right in cortex samples, highlighted by the gradient of colors with age from light to dark, respectively (Fig. 2B). To determine if the Arctic model has sex-specific effects, we used edgeR [30] to identify differentially expressed genes between male and female Arc mice. Genes upregulated in females were mainly those known to be sexually dysmorphic genes [35], such as Xist and Tsix, which are located on the X-chromosome, whereas males presented upregulation of genes known to be male-specific, such as Eif2s3y and Ddx3y, which are located on the Y-chromosome (Additional file 1: Fig S4A, B). Therefore, differential expression analyses showed lack of sex-specific changes in the hippocampus and cortex of Arc mice at all ages.
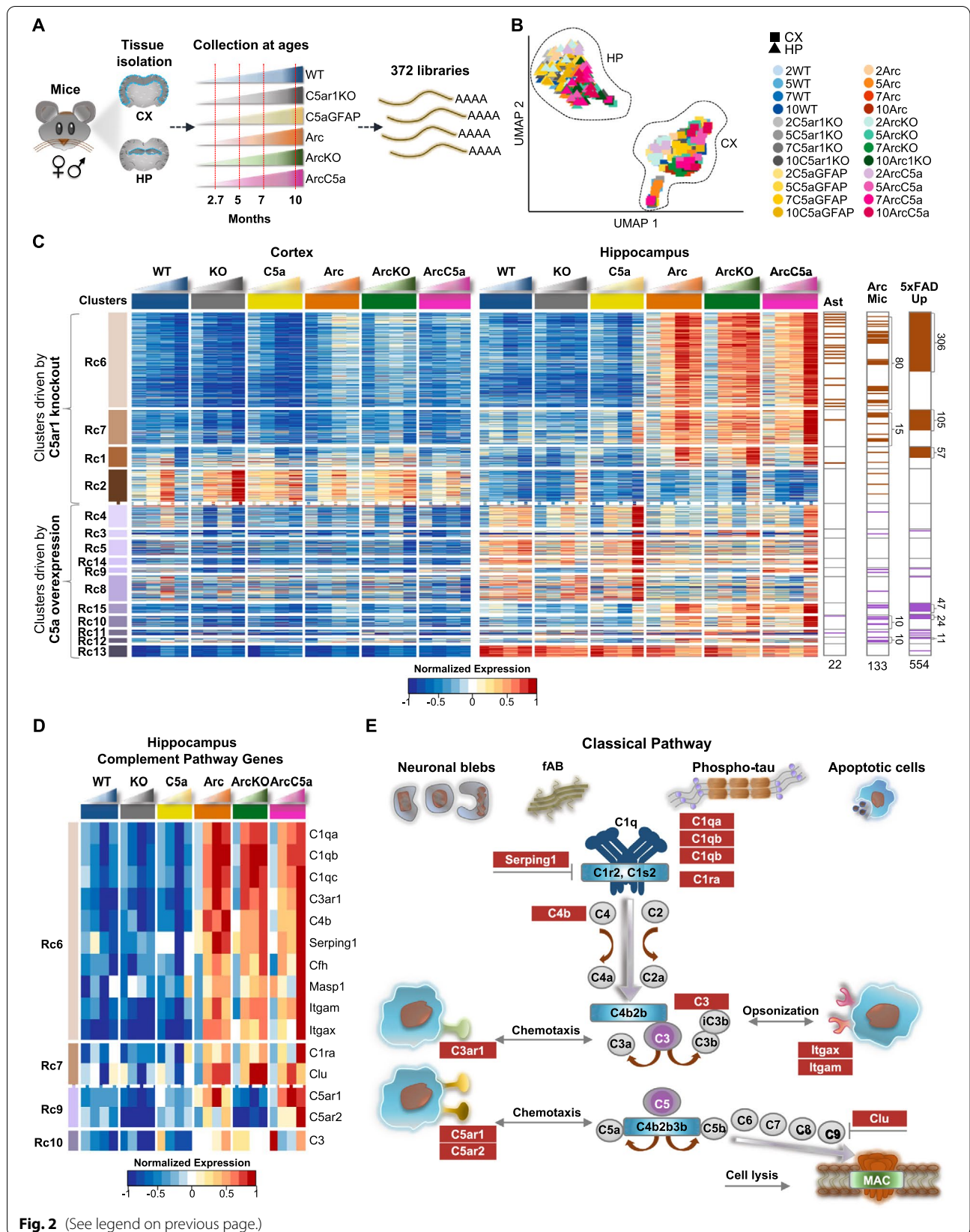
Using maSigPro (Additional file 1: Fig S5A) [32], we identified 1763 genes whose expressions varied in a time-specific fashion. These genes grouped into 15 RNA clusters with distinct patterns of expression (Fig. 2C). RNA cluster (Rc)6, Rc7, Rc1, and Rc2 represent genes whose expression changes were mainly driven by the knockout of C5ar1 and are represented in shades of brown. Rc4, Rc3, Rc5, and Rc8 to Rc15 represent genes whose expression changed mainly in response to C5a overexpression and thus are represented in shades of lilac. Each cluster contains distinct subsets of complement pathway (CP) genes, as well as distinct subsets of astrocyte-associated (Ast) [19], Arc microglia-associated (Arc Mic) [18], and AD-associated genes elevated in the 5xFAD mouse model with pathology (5xFAD up) [36] (Fig. 2C and Additional file 1: Fig S5B, C). Expression of the C5ar1 gene was induced in Arc relative to WT as early as 2.7 months and increased more dramatically at 5 and 7 months, while was lowest (essentially non detectable) in the C5aR1KO and ArcC5aR1KO cohorts, confirming its genetic ablation (Fig. 2D). Expression of C5ar2 was also decreased in the C5aR1KO and ArcC5aR1KO cohorts, consistent with previous studies showing a correspondence in expression of those genes [37, 38], but strongly induced in the ArcC5a+ particularly at 10 months. The ArcC5a+- and ArcC5aR1KO-dependent expression changes in Rc6, Rc7, and Rc1 were more abundant in the hippocampus compared to cortex, correlating with the relative density of amyloid pathology in the Arc mice (Additional file 1: Fig S6C), and thus suggesting synergy/interaction between the presence of amyloid plaques and C5aR1 signaling. Thus, we focused our analysis of RNA-seq on the hippocampus, where pathology is consistently more pronounced.

Expression of genes of some of the early complement pathway components were induced in Arc mice with a peak at 7 months of age and suppressed in the absence of C5ar1. Notably, cluster Rc6 contained most of the complement genes identified using maSigPro including C1qa, C1qb, C1qc (known to be coordinately expressed) [39, 40], and C4b (designation for the mouse C4 gene),

---

(See figure on next page.)

Fig. 2 Distinct subsets of genes in the hippocampus are affected by C5ar1 knockout or C5a overexpression. **A** Schematic diagram of experimental design highlighting 372 RNA-seq samples processed from cortices and hippocampi of 6 mouse genotypes during disease progression at 2.7, 5, 7, and 10 months of age. **B** UMAP embedding representation of 372 RNA-seq samples represented in **A**. Samples separated out mostly by tissue type (hippocampus (HP) and cortex (CX)). Samples from WT mice are represented in shades of blue, from the C5ar1KO cohort in shades of gray, from the C5aGFAP cohort in shades of yellow, from the Arctic cohort in shades of orange, from the ArcC5ar1KO cohort in shades of green, and samples from the ArcC5aGFAP cohort in shades of pink. **C** Heatmap of 1763 genes with dynamic temporal profiles in the hippocampus identified by maSigPro clustering (alpha < 0.05, FDR < 0.05%). Each column represents the average expression for a time point and each row represents a gene. Each cluster represents a subset of genes that show a similar pattern of expression along the time-course in the hippocampus. Clusters shown in brown gradient and lilac gradient (far left) represent genes whose expression changes are driven by C5ar1KO or C5a overexpression, respectively. RNA-seq data (TPM) is row-mean normalized. Astrocyte-associated genes (Ast), genes upregulated in microglia isolated from Arctic mice (Arc Mic), and genes upregulated with pathology progression in the 5xFAD mice (5xFAD Up) present in each cluster are shown (far right). **D** Heatmap of 15 genes of the complement pathway expressed in hippocampal samples that were present in maSigPro identified clusters. RNA-seq data (TPM) is row-mean normalized. **E** Representative diagram of the Classical pathway activation of the complement cascade, highlighting complement-associated genes present in the maSigPro identified clusters (as seen in panel **D**). $N = 4$–10 mice/genotype/age

Carvalho *et al. Journal of Neuroinflammation*   (2022) 19:178

Page 7 of 21

Fig. 2 (See legend on previous page.)

Carvalho *et al. Journal of Neuroinflammation*   (2022) 19:178

Page 8 of 21

as well as the receptor for the C3a activation fragment, C3ar1, and the inhibitor Serping1 (inhibitor of C1, as well as bradykinin formation), all of which showed higher expression in the Arc mice at 5 months and increasing with age (Fig. 2D). The earliest upregulated complement related genes in Arc relative to WT were C5aR1, C4b, Serping1 and C3 as well as C1q, and C3ar1 at 2.7 months of age. While C1q was robustly upregulated in all Arc genotypes, consistent with the rapid increase in multiple other injury models, increases in expression of the genes for C4 (required for synaptic pruning), Factor H and Serping1 were slower in the ArcC5aR1KO as seen in the previous analysis of isolated microglia in this model [18]. Interestingly, delayed increases in these components were also seen in ArcC5a+, but by 10 months expression levels of these genes reached or surpassed that seen in the Arctic.

Additional changes in expression of complement genes were driven by transgene overproduction of C5a. Complement genes Masp1 and C1ra, regulators Cfh and Serping1, and the α chains Itgam (CD11b) and Itgax (CD11c) of CR3 and CR4, respectively, were upregulated early by the presence of the Arctic APP transgene but showed increased expression in the ArcC5a+ hippocampus at 10 months (Fig. 2D). Thus, the expression of individual complement genes may be orchestrated to fit the local environment with the knockout of C5aR1 and the overexpression of C5a affecting the level and time of induction of genes that act in multiple arms of the complement cascade, including complement factors, receptors, and inhibitors (Fig. 2E).

C5aR1 ablation may delay microglial switch from disease mitigating to disease enhancing

To understand the effects of C5a–C5aR1 signaling on gene expression in AD, changes in expression of genes found in the current bulk RNA analysis were compared to our previous reports of microglia isolated from combined cortex and hippocampus from Arc and ArcC5aR1KO at the same ages [18], to those known to be associated with AD pathology progression in the 5xFAD mice model [36], and to human AD genes, such as Cd33, Trem2, Tyrobp, Inpp5d, and S100a6 [41–44] (Fig. 2C, right and Additional file 1: Fig S5B). Most of the genes upregulated in previously assessed microglia isolated from the Arc mice were part of clusters Rc6 (80 genes) and Rc7 (15 genes),

which are linked to inflammation and cholesterol metabolism, respectively (Fig. 2C). Similarly, most of the genes upregulated in the brain of the 5xFAD mouse model were part of Rc6 (306 genes) and Rc7 (105 genes). While many genes were upregulated with accumulation of amyloid regardless of C5a–C5aR1 status, human AD genes Cd33, Trem2, Tyrobp and Cst7 (Fig. 3A) showed increased expression in the Arc cohort with a peak at 7 months of age. However, the ArcC5aR1KO the expression increased at a lower rate and did not peak until 10 months of age. Inpp5d, whose expression is increased in human LOAD, showed lower expression at all ages in the ArcC5aR1KO (Fig. 3A and Additional file 1: Fig S5B). It has been shown that Inpp5d expression increases in early stages of AD in Japanese patients, is positively correlated with plaque load in LOAD [45] and increases with progression of disease in the 5xFAD mouse model [46]. Similarly, S100a6 is upregulated in patients with AD, as well as AD mouse models [47]. Stat3 has been associated with worsening cognitive decline in the 5xFAD mice [48]. Thus, C5ar1 deletion either delayed or prevented the expression of several genes upregulated in the Arctic and 5xFAD mouse models and human AD. In summary, eliminating C5ar1 in the Arctic AD model results in a decrease or delay of expression of many, but not all, reactive glial genes associated with AD in human or mouse models, indicating a separation between those genes induced by amyloid plaques (or other sources of "damage") and those requiring the C5a–C5aR1 signaling.

C5a–C5aR1 signaling influences astrocyte activation

While many of the above genes are considered predominantly microglial genes, given the evidence for altered astrocyte states in AD [19, 49, 50], we investigated the changes in expression of astrocyte-associated genes. Rc6 contained 18 astrocyte-associated genes, including pan-reactive astrocyte genes Lcn2, Osmr, Cd44, Vim, and Serpina3n and A1 reactive astrocyte genes Ggta1, H2-T23, Srgn, and Serping1 [19], whose expression was higher in the Arc cohort. Ablation of C5ar1 reduced or delayed the activation of those genes (Additional file 1: Fig S5C), suggesting that C5ar1 deletion may reduce the activation of neurotoxic reactive astrocytes. Interestingly, overexpression of C5a led to increased expression of these pan-reactive and A1 genes at 10 months suggesting that an increase in C5a may lead to activation of primed reactive

(See figure on next page.)
Fig. 3 Delay and/or reduction of inflammation- and DAM-associated genes in the ArcticC5aR1KO hippocampus. **A** Heatmap of selected genes in the hippocampus present in RNA cluster 6. Genes were clustered based on AD study findings and molecular functions. RNA-seq data (TPM) is row-mean normalized. **B** Gene ontology (GO) and pathway enrichment analyses of genes present in Rc6. **C** Heatmap of genes enriched in Phagosome pathway (mmu04145) in the hippocampus. Numbers in front of gene names correspond to protein they encode, as seen in **D**. **D** Representative diagram of the Phagosome pathway (mmu04145) with select protein encoded by genes present in the panel **C** heatmap highlighted in red. *N* = 4–10 mice/genotype/age
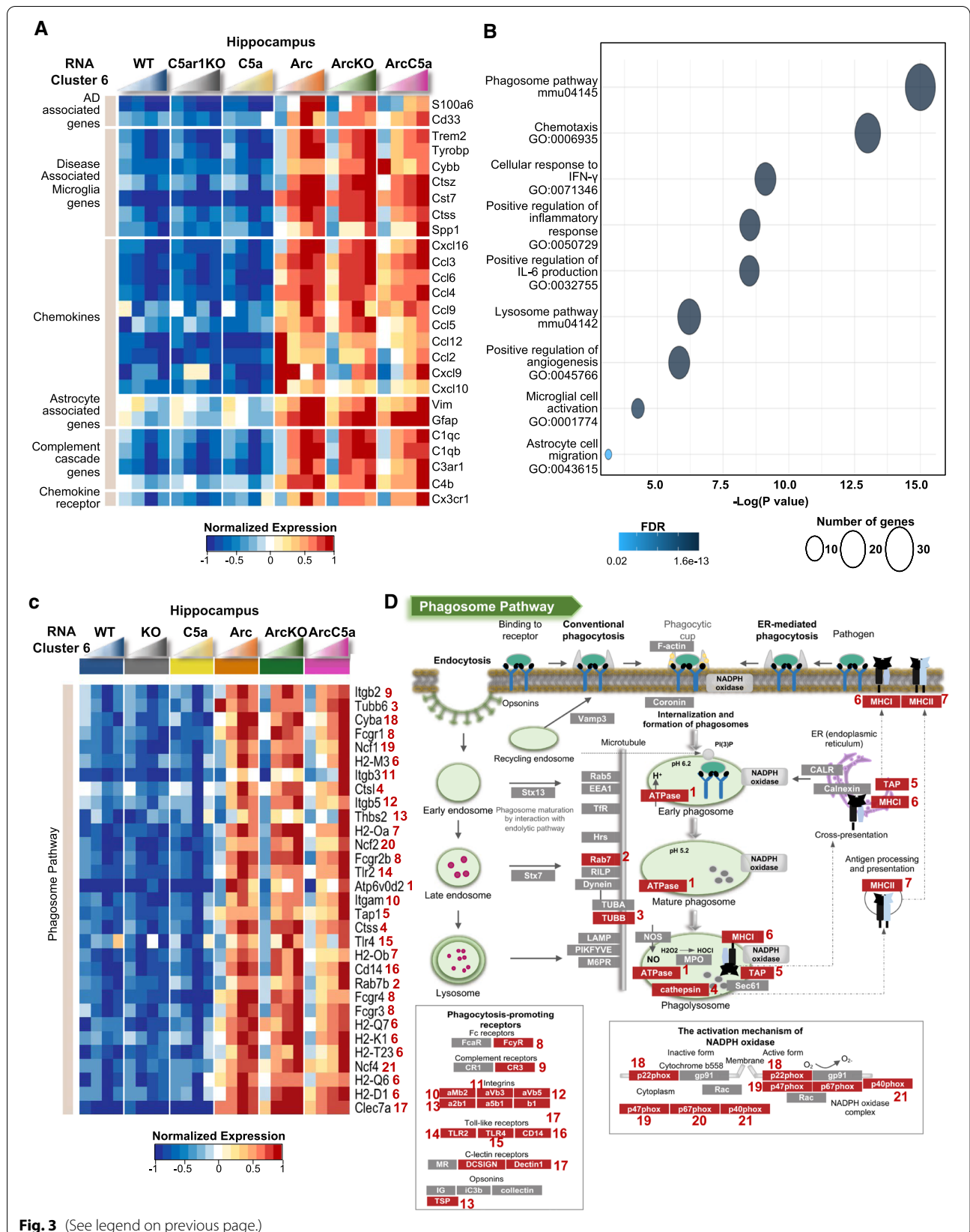
Carvalho *et al. Journal of Neuroinflammation* (2022) 19:178

Page 9 of 21

Fig. 3 (See legend on previous page.)

Carvalho *et al. Journal of Neuroinflammation*   (2022) 19:178

Page 10 of 21

astrocytes, either directly or indirectly. GFAP (pan-reactive) and Aspg and Psmb8 (A1) were highly upregulated in the presence of amyloid plaques regardless of C5a–C5aR1 manipulation, indicating a subset of astrocyte genes that are responsive to insult, but not influenced by C5aR1 signaling (Additional file 1: Fig S5C). Assessing the microglial mediators of astrocyte activation, TNFα, IL1α and C1q [19, 51], we found that while IL1α was elevated at 5 months in the ArcC5aR1KO relative to Arc and ArcC5a+, TNFα expression was substantially delayed in ArcC5ar1KO, and C1qa-c were transcribed with the same temporal increase in response to plaque accumulation for all Arc genotypes (Fig. 2D, Additional file 1: Fig S5B, D). These findings indicate a complexity of astrocyte response mediators that are induced by different insults or injury and demonstrate that expression levels of some powerful mediators can be modulated by C5a–C5aR1 signaling.

Gene ontology analysis of Rc6 revealed reduced expression of inflammation- and DAM-associated genes in the ArcC5aR1KO mice

We performed gene ontology analysis to identify relevant biological processes and pathways associated with differentially expressed genes present in each maSigPro cluster. Expression of genes in Rc6 was higher in Arc mice and peaked in the hippocampus of the Arc cohort at 7 months. However, in the ArcC5a+ cohort, expression did not increase until 10 months of age. Rc6 was enriched for DAM genes, such as Trem2, Tyrobp, Cybb (gp91 of the NADPH oxidase), Cst7, Ctss, and Spp1 (Fig. 3A and C). Rc6 also contained inflammatory chemokine genes such as Ccl12, Ccl2, and Cxcl10 that were highly expressed in the Arc at 2.7 months before dropping and then slowly increasing. Neither ArcC5aR1KO nor ArcC5a+ expressed these genes at 2.7 months prior to plaques deposition. Additionally, gene ontology and pathway analysis showed enrichment for biological processes that are significant in the AD context, for instance regulation of inflammatory signaling including IFN-γ and IL-6 production, as well as microglial cell activation and lysosome pathway, all of which were delayed in the ArcticC5aR1KO cohort (Fig. 3B). Our results suggested that the ablation of C5ar1 delayed disease-enhancing activation genes without diminishing the disease-mitigating response to injury (Fig. 3C).
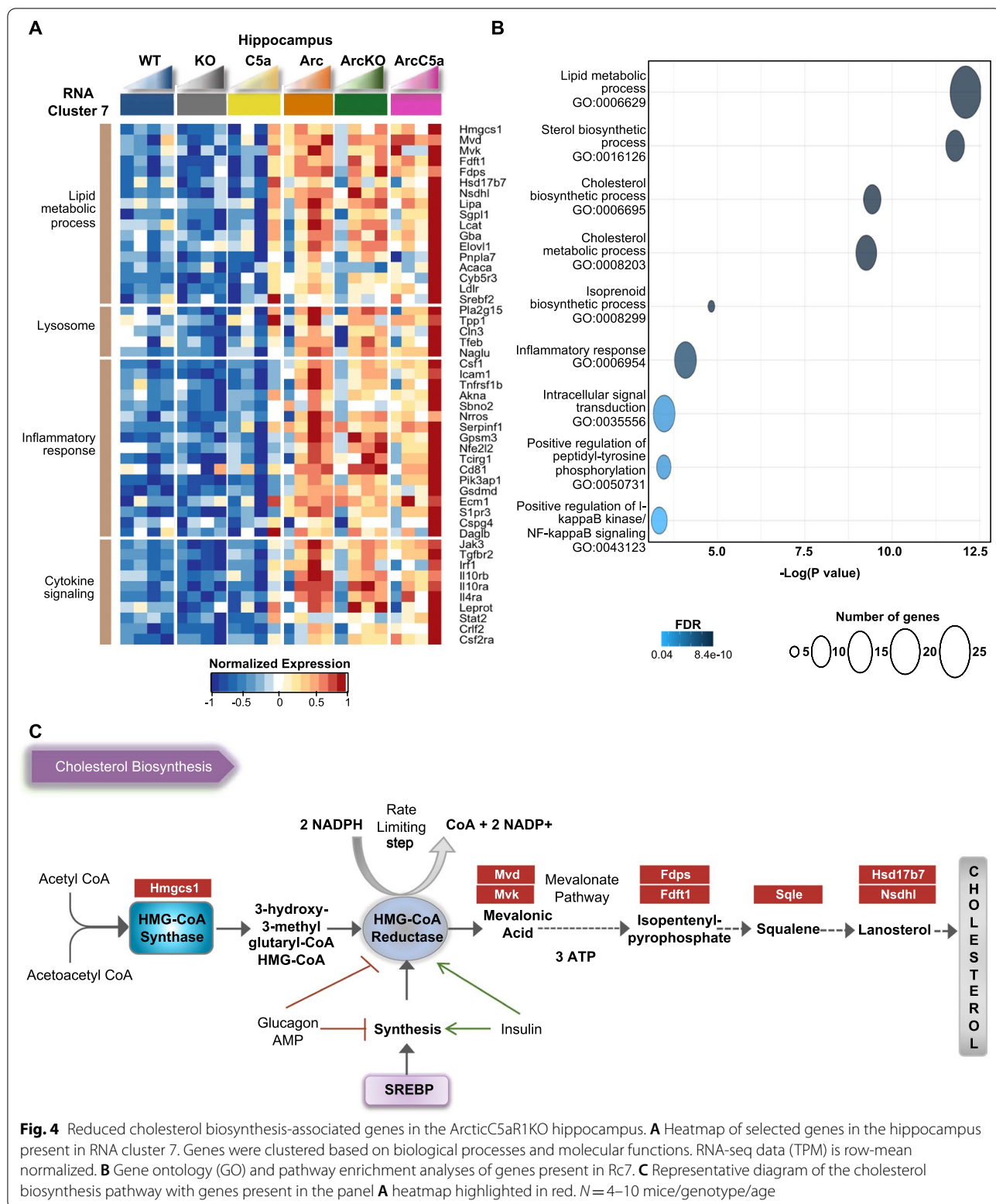
Gene ontology analysis of Rc7 revealed reduced expression of genes associated with lipid and cholesterol biosynthesis and metabolism in the ArcC5aR1KO mice and increased expression of genes of those genes in the ArcC5a+ mice
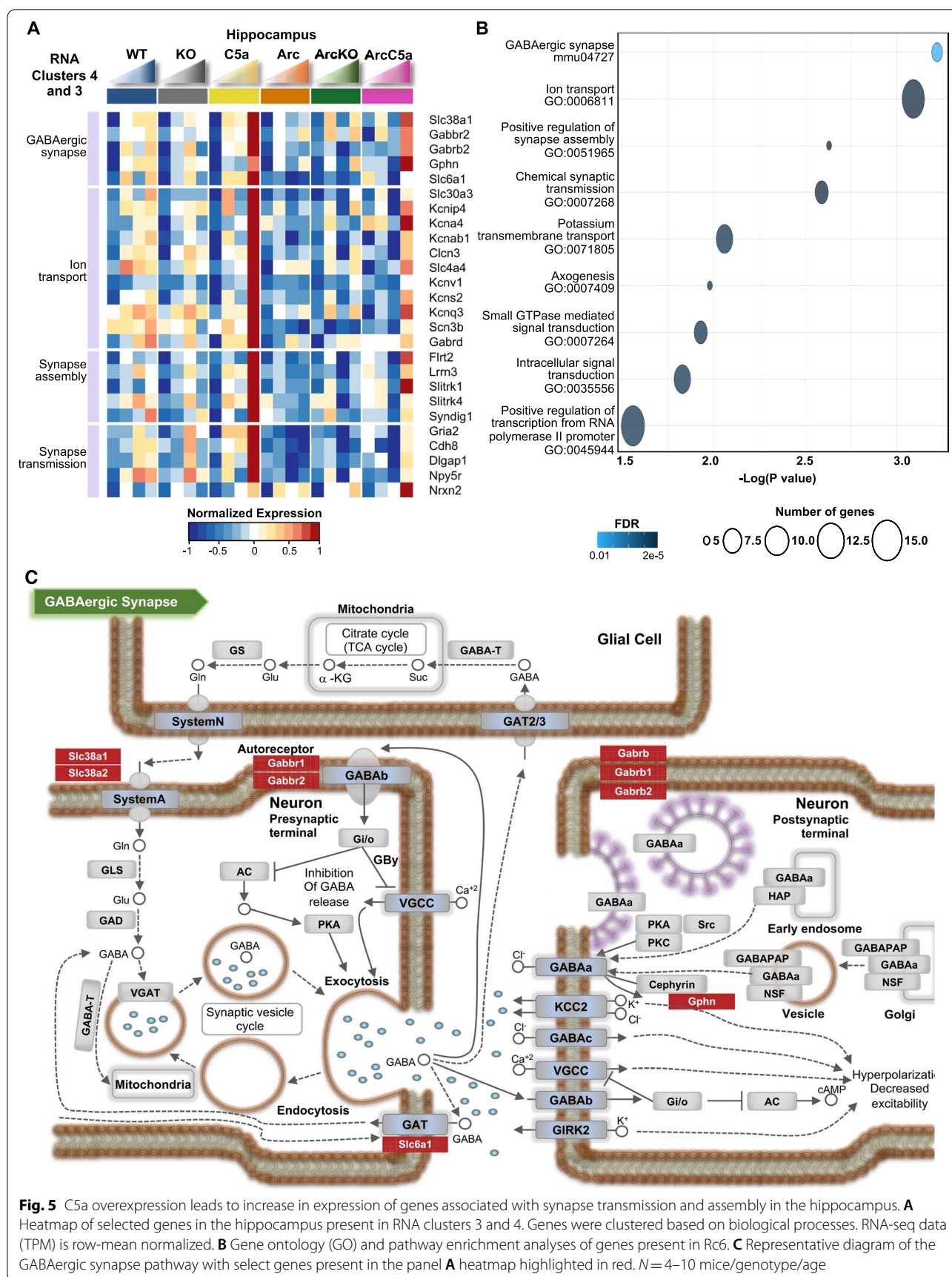
Rc7 mainly consisted of genes whose expression was increased in the Arc peaking at 7 months. While expression in the ArcC5aR1KO remained higher than C5aR1KO controls, it did not increase uniformly with age. Interestingly, genes in Rc7 were highly upregulated in the ArcC5a+ mice at 10 months compared to earlier ages and Arc and ArcC5aR1KO (Fig. 4A). Rc7 also contained genes associated with inflammatory response, such as Csf1, Icam1, Tnfsf1b, Akna, Sbno2, and Nrros and cytokine signaling, such as Jak3 and receptor Tgfbr2, whose expressions were reduced in the absence of C5ar1. Gene ontology and pathway analysis showed enrichment for lipid metabolic processes, inflammatory response, and cholesterol biosynthesis, suggesting that those processes were induced by amyloid plaque challenge, but reduced upon C5ar1 deletion in the Arctic model at 7 months while upregulated at 10 months when C5a is overexpressed (Fig. 4A, B). Cholesterol cannot cross the blood–brain barrier, and thus almost all brain cholesterol is synthesized locally. Interestingly, many of these genes are also upregulated in the C5a+ in the absence of the APP transgene at 10 months of age. Our results suggest that ablation of C5ar1 reduces brain cholesterol metabolic processes or the need for such processes, and that cholesterol metabolism in the brain may be partially influenced by high concentrations of C5a (Fig. 4C).

C5a overexpression leads to increased expression of genes associated with synapse transmission and assembly

C5a has been shown to promote neuronal damage in vitro [8], although it plays a positive role in neurogenesis during early development [52]. We thus sought to explore effects of C5a overexpression in our mice in the presence and absence of amyloid pathology, given the accelerated behavior deficiency in the ArcC5a+ mice relative to the Arc at 10 months. In clusters 3 and 4, there was a general decrease with age in the Arc mice relative to the wild-type controls, except for a marked increase in ArcC5a+ mice at 10 months, but an even greater increase in gene expression in the C5a+ mice at 10 months in the absence of the amyloid transgene (Fig. 5A). C5a overexpression promoted pathways associated with GABAergic synapses, ion transport, synapse assembly, axogenesis, and transcription (Fig. 5B), more so in the absence of the Arc transgene. Specifically, C5a overexpression was associated with an increase of genes that regulate GABAergic synapse processes (Fig. 5C). It has been shown that alterations of GABAergic neurotransmission may contribute to AD pathology [53, 54]. Therefore, C5a overexpression might contribute to alterations of GABAergic transmissions independently of amyloid pathology. Whether these aberrant synaptic processes are associated with the acceleration of cognitive decline in ArcC5a+ mice is yet to be explored.

Fig. 4 Reduced cholesterol biosynthesis-associated genes in the ArcticC5aR1KO hippocampus. **A** Heatmap of selected genes in the hippocampus present in RNA cluster 7. Genes were clustered based on biological processes and molecular functions. RNA-seq data (TPM) is row-mean normalized. **B** Gene ontology (GO) and pathway enrichment analyses of genes present in Rc7. **C** Representative diagram of the cholesterol biosynthesis pathway with genes present in the panel **A** heatmap highlighted in red. N = 4–10 mice/genotype/age

Carvalho *et al. Journal of Neuroinflammation* (2022) 19:178

Page 12 of 21

Fig. 5 C5a overexpression leads to increase in expression of genes associated with synapse transmission and assembly in the hippocampus. **A** Heatmap of selected genes in the hippocampus present in RNA clusters 3 and 4. Genes were clustered based on biological processes. RNA-seq data (TPM) is row-mean normalized. **B** Gene ontology (GO) and pathway enrichment analyses of genes present in Rc6. **C** Representative diagram of the GABAergic synapse pathway with select genes present in the panel **A** heatmap highlighted in red. $N = 4$–10 mice/genotype/age

Modulation of microglia activation marker CD11c in Arctic mice by C5a signaling

Amyloid pathology in humans and animal models can activate microglia to an inflammatory and disease-enhancing state [55]. We observed evidence of a delay in some phagosome and inflammatory pathways driven by elimination of C5aR1 and an exacerbation driven by

overexpression of C5a at 10 months in the RNA-seq data. To determine the effects of C5aR1 ablation or C5a overexpression on amyloid-associated microglial protein expression, we stained ArcC5aR1KO and ArcC5a+ tissue with antibodies for CD11b and CD11c and compared levels to Arctic at 5, 7, and 10 months (Fig. 6). The hippocampus and cortex were assessed separately
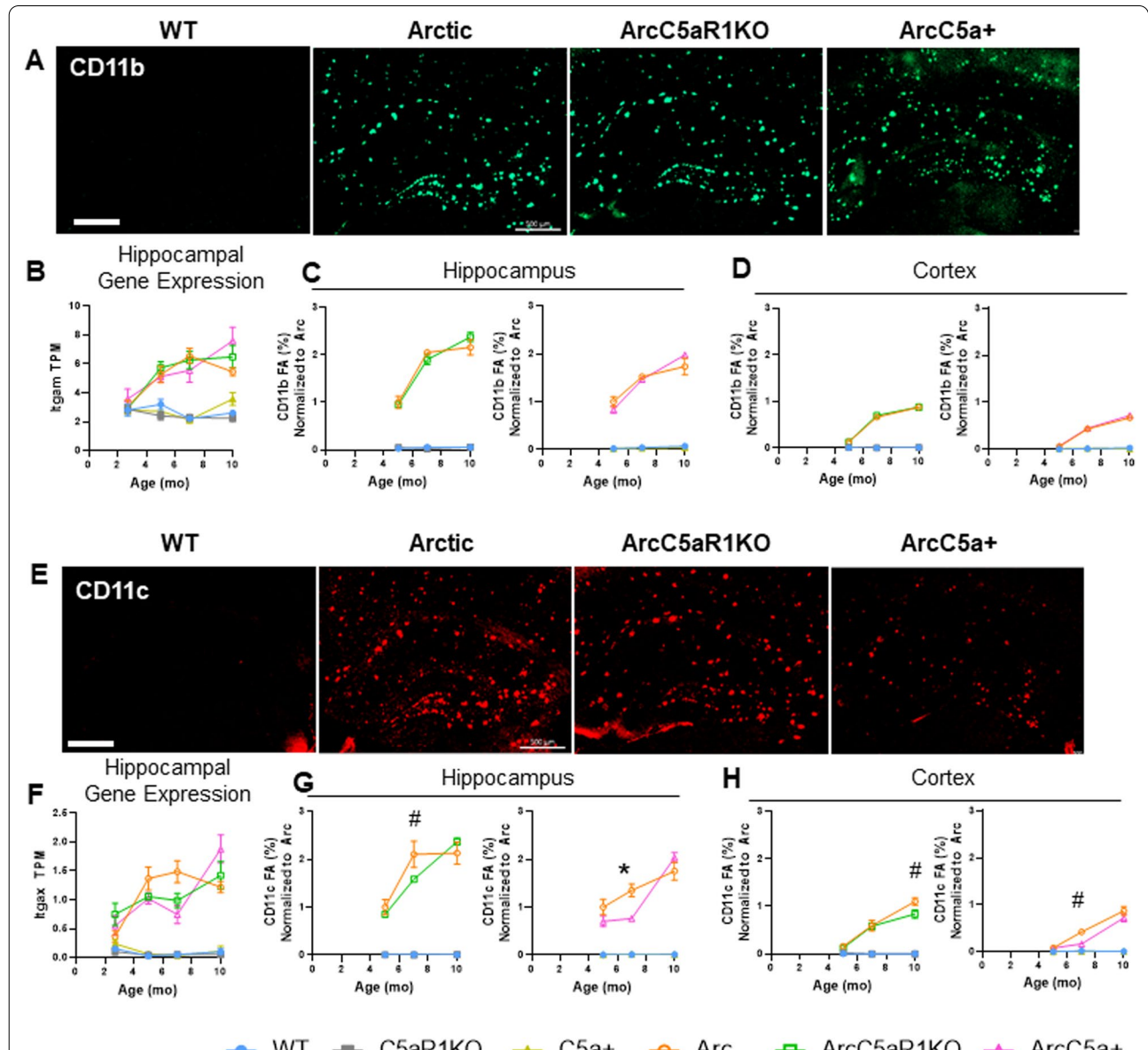
Fig. 6 CD11c expression changes with C5a overexpression or C5aR1 ablation. **A** Representative images from 7 months of CD11b positive microglia in WT, Arctic, ArcticC5aR1KO, and ArcticC5a+ in the hippocampus. **B–D** Quantification of gene expression (TPM) of *Itgam* in the hippocampus (**B**) and percent field area of CD11b in hippocampus (**C**) and cortex (**D**) at 5, 7, and 10 months. **E** Representative images from 7 months of CD11c-positive microglia in WT, Arctic, ArcticC5aR1KO, and ArcticC5a+ in the hippocampus. **F–H** Quantification of gene expression (TPM) of *Itgax* in the hippocampus (**F**) and percent field area of CD11c in hippocampus (**G**) and cortex (**H**) at 5, 7, and 10 months. C5aR1KO and C5a+ cohorts were stained and analyzed separately. Four sections were stained per mouse and the percent field area was averaged over the 4 data points. Data shown as mean ± SEM. *$p < 0.05$, #$0.1 > p > 0.05$. Two-way ANOVA with Tukey's post hoc test. $N = 2$–6 mice/genotype/age. Scale bar 500 µm

Carvalho *et al. Journal of Neuroinflammation*   (2022) 19:178

Page 14 of 21

as amyloid deposition and glial activation are seen first, and to a larger extent, in the hippocampus compared to the cortex in the Arc model (Additional file 1: Fig S6A, B). As previously noted, amyloid deposition in the hippocampus remained essentially unchanged with deletion of C5aR1 or overexpression of C5a, with only small changes detected in the ArcC5aR1KO CA1 hippocampal region in one cohort a 7 months of age (Additional file 1: Fig S6C–F and [18]).

CD11b is part of the integrin receptor, CR3, with multiple ligands including iC3b/C3b. It is expressed exclusively on microglia in the CNS [56], and previously shown to be upregulated in AD models [57, 58]. As expected, CD11b levels were elevated in the hippocampus (Fig. 6A, C), and to a lesser extent in the cortex (Fig. 6D), of Arc, ArcC5a-R1KO, and ArcC5a+ mice compared to their respective controls. CD11b levels peaked at 7 months in the Arc hippocampus, and plateaued thereafter, paralleling our findings from RNA-seq data (Fig. 6B). While in some cohorts CD11b was lower in ArcC5aR1KO at 7 months, the increase in CD11b was correlated with amyloid load and not downstream complement activation.

CD11c-positive microglia appear early in response to plaque deposition and continue to increase with disease progression around plaques in APP/PS1 mice [59]. A time-course of CD11c expression and immunoreactivity (Fig. 6E, G, H) revealed that while essentially absent in the WT, C5aR1KO, and C5a+ genotypes at all ages, CD11c levels increased with age/disease progression in the hippocampus and cortex of Arc, ArcC5aR1KO, and ArcC5a+ mice (Fig. 6G, H). While CD11c levels were significantly elevated in the Arc hippocampus at 5–10 months compared to controls, we observed 25% and 43% lower CD11c levels in the ArcC5aR1KO and ArcC5a+ hippocampus, respectively, compared to Arc at 7 months (Fig. 6G). Furthermore, ArcC5a+ mice had 60% lower CD11c in the cortex at 7 months compared to Arc mice (Fig. 6H). Interestingly, hippocampal CD11c levels increased to Arc levels by 10 months of age in both ArcC5aR1KO and ArcC5a+. The temporal changes in hippocampal CD11c protein levels in Arc, ArcC5aR1KO, and ArcC5a+ mice match the temporal profile of Itgax gene expression detected with RNA-seq (Fig. 6F). These findings suggest that blocking C5aR1 may delay or reduce the polarization of a subset of reactive microglia from an early-intermediate stage to a later stage of reactivity in the Arctic model. Thus, appearance of CD11c+ microglia surrounding the plaques may be a key biomarker of microglia that ultimately indicates directly or indirectly cognitive decline and neurodegeneration.

We further assessed pan-reactive and lysosomal markers Iba1 and CD68 (Additional file 1: Fig S7). Iba1 levels were consistently elevated in Arc, ArcC5aR1KO, and ArcC5a+ hippocampus compared to controls (Additional file 1: Fig S7A, D, E). At 5 months, Iba1 field area was slightly lower in ArcC5a+ compared to Arc, but by 7 months levels were comparable in all three Arc genotypes (Additional file 1: Fig S7D). CD68 levels were higher in all Arc groups in the hippocampus and to a lesser extent in the cortex compared to WT groups as early as 5 months, matching RNA-seq data (Additional file 1: Fig S7B, F–H).

Astrocyte markers GFAP and C3 are largely unaltered by C5aR1 engagement in the hippocampus

A recent study demonstrated that inflammatory cytokines released by microglia can trigger a shift towards neurotoxic reactivity in astrocytes [19]. Thus, to complement the RNA-seq data, we used immunohistochemistry for the pan-reactive astrocyte marker GFAP as well as C3, whose expression has reproducibly been shown to be elevated in neurodegenerative models [19, 60], to characterize changes in astrocyte polarization with disease progression and modulation of C5a–C5aR1 signaling. As expected, we observed a significant increase in GFAP and C3 percent field area in all three Arc groups compared to WT controls in the hippocampus and cortex (Additional file 1: Fig S8A). Transgene expression of C5a did not significantly change GFAP levels in the CA1 or DG of the hippocampus (Additional file 1: Fig S8C–E), but did result in decreased levels of GFAP in the CA3 hippocampal region at the early stages of disease (5 months) relative to Arc mice and a reduction relative to C5aR1-sufficient Arc in cortex at 7 months of age, although the reduction of expression was greater in the C5aR1-deficient Arc cortex at that age (48% reduction) (Additional file 1: Fig S8F). C3 expression was variable in hippocampal regions with 39% ($p < 0.05$) decrease in C3 volume in CA1 in ArcC5aR1KO relative to Arc at 7 months of age (Fig. 7), while a decrease of 83% of C3 volume and 43% of C3 Field area % were noted in the cortex in two different cohorts of ArcC5aR1KO, relative to Arc mice at 7 months of age (Fig. 7, Additional file 1: Fig S8B, J). Lower C3 was seen in the CA1 of ArcC5a+ mice at 7 months, but, as in ArcC5aR1KO, by 10 months C3 reactivity was not different from Arc genotype. These data support that ablation of C5aR1, and to a lesser extent C5a overexpression, results in a delay in amyloid-induced astrocyte polarization.

Discussion

Using genetic ablation of C5aR1 and transgenic overexpression of the ligand C5a in wild type and Arctic AD model mice, we provide a characterization of cellular, molecular, and transcriptomic changes that occur throughout disease progression and that are modulated

Carvalho *et al. Journal of Neuroinflammation*   (2022) 19:178

Page 15 of 21
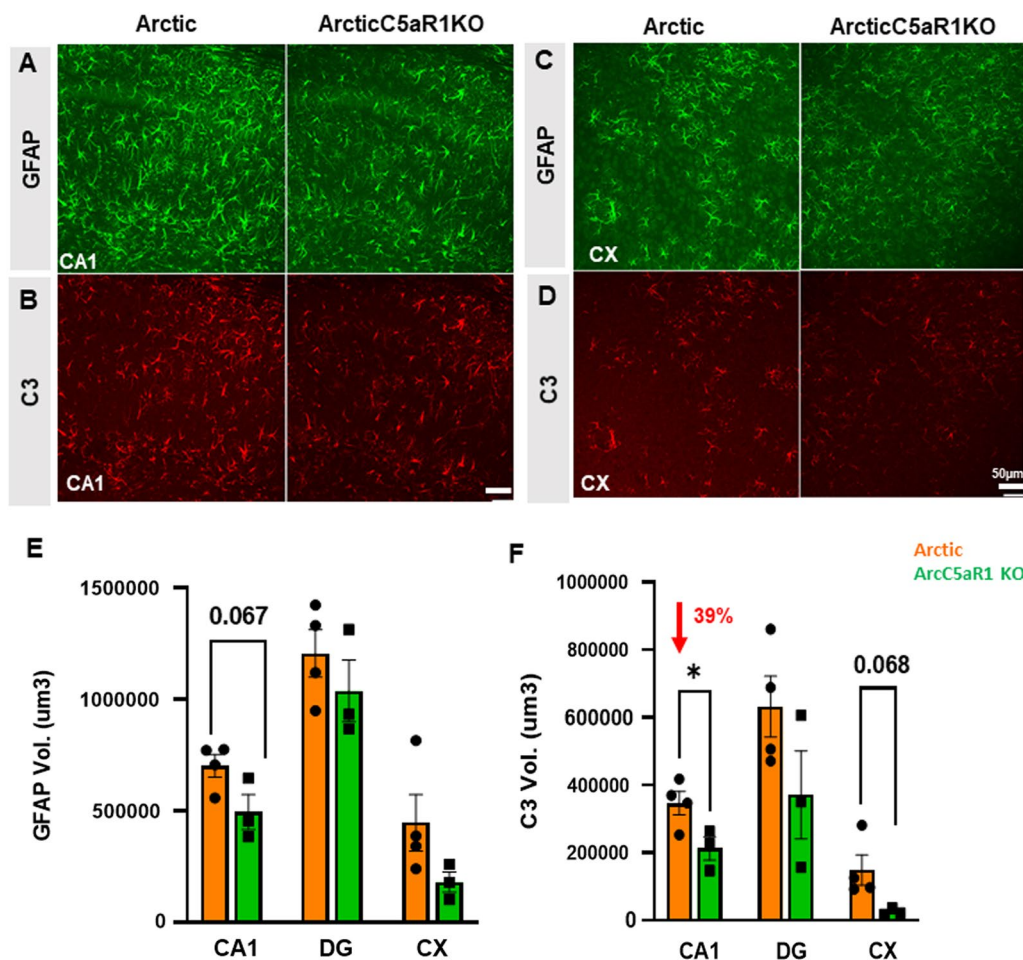
Fig. 7 Lower astrocyte C3 expression in ArcticC5aR1KO compared to Arctic mice. Representative confocal images of GFAP immunostaining in the hippocampal cornu ammonis 1 (CA1) region (**A**) and in cortex (CX) (**C**) region and C3 immunostaining in the CA1 region (**B**) and in CX region (**D**) of Arc and ArcC5aR1KO brain at 7 months of age. Quantification of GFAP (**E**) and C3 (**F**) volume in the CA1, DG and CX. Z stack (31 steps, 30 um) one area/region (confocal Leica SP8, 20×). Data shown as mean ± SEM. *$p < 0.05$. *T*-test. $N = 3$–4 mice/genotype. Scale bar 50 μm

by C5aR1 activation in the Arctic mouse model of AD. Further support of a detrimental role of C5a–C5aR1 signaling in the Arctic mouse is shown by the acceleration of hippocampal-dependent spatial memory deficits by overproduction of C5a by a transgene under the GFAP promoter. The upregulated profiles of complement proteins in AD brain [61–63] and the demonstrated safety of the suppression of C5a generation or C5aR1 signaling in human patients with inflammatory diseases [64, 65], suggests C5aR1 antagonism would be well tolerated and may slow cognitive decline in AD and other neurodegenerative diseases in which complement activation is excessive or not appropriately regulated.

For the past decade or so, evidence has been accumulating for a role of the complement system in neuronal injury, synaptic pruning, and cognitive decline [66–69]. In the healthy developing brain, complement proteins tag extranumerary synapses or cellular debris for clearance by microglia [68]. However, aberrant complement activity may result in the removal of synapses from stressed neurons in neurodegenerative diseases [70]. Complement proteins are upregulated in the human and mouse brain with normal aging and are further increased in AD, models of AD and other neurological diseases [5, 61]. Deletion of C1q, C3, or CR3 (CD11b/CD18) reduces microglial engulfment of synapses [68, 71, 72] and protects against memory deficits in aged mice [73] and in models of AD [70, 74] and other neurological disorders (reviewed in [75]). While some have suggested inhibition of upstream complement components (such as C1, C3 and CR3) as a therapeutic strategy, a potential improvement on this strategy would be a more targeted inhibition of the downstream complement activation products, such as the pro-inflammatory fragment C5a, to preserve

the immunoprotective functions of the upstream molecules. For example, C1q can be beneficial by binding to apoptotic neurons to promote clearance by microglia to maintain neuronal homeostasis [76]. Previous studies have shown that pharmacologic inhibition or genetic ablation of C5aR1 protects against learning and memory deficits in several mouse models of amyloidosis [9, 18] and that C5a contributes to neuronal injury [7, 8]. Landlinger and colleagues provided evidence for a protective effect of an active immunization against C5a in the Tg2576 mouse model of AD, with suppression of CD45^{hi} microglia in immunized mice and some improvement in contextual memory [77]. Thus, inhibition of the C5a–C5aR1 pathway could reduce myeloid cell activation as demonstrated here, without interfering with upstream beneficial complement signaling or the formation of the downstream beneficial pathogen killing membrane attack complex [18].

The Arctic 48 mutation results in an altered Aβ peptide sequence (E22G) that drives rapid fibril formation and resilience to degradation, resulting in aggressive fibrillar plaque accumulation [78]. Using this model, our previous work demonstrated that amyloid is a necessary but not the sole driver of cognitive decline [18], as ablation of C5aR1 prevented loss of neuronal complexity and cognition. Here, our RNA-seq data demonstrated that C5a+- and C5aR1KO-dependent changes in gene expression in the brains of Arctic mice were more prominent in the hippocampus compared to the cortex (with the exception of Rc2) correlating with amyloid load and the significance of hippocampal region on memory and cognition. Eliminating C5aR1 from the Arctic mice did not alter amyloid plaque accumulation, but did delay or reduce expression of genes enriched for inflammatory signaling pathways and microglial cell activation, and several other important AD-associated genes in the hippocampus. Not all AD-associated genes were altered, indicating differences in genes whose expression change in response to amyloid plaque deposition and genes whose expression change in response to C5a–C5aR1 signaling, the latter of which may play an essential role in worsening AD cognitive performance. For example, eliminating C5aR1 reduced expression of Inpp5d (SHIP1), which reduces phagocytic capabilities in plaque-associated microglia [45], S100a6, which is found in plaque-associated astrocytes [79], and Stat3, which induces astrocyte reactivity in the 5xFAD model and astrocyte-mediated pro-inflammatory cytokine release in the APP/PS1 model [48, 80], all of which are upregulated and appear to play a detrimental role in human AD brain or mouse models of AD. Arctic mice displayed higher levels of several pattern recognition receptor (PRR) genes, such as Tlr2, Clec7a (Dectin-1), Ifih1 (MDA5), Ddx58 (Rig-1), and Nlrp10),

particularly in the hippocampus at 7 and/or 10 months of age. Although C5a signaling has been shown to modulate PRR [81–83], in the present study, C5a overexpression or C5aR1 ablation did not significantly alter the expression patterns of these genes. This suggests that there are C5a–C5aR1-independent, perhaps amyloid-dependent, pathways of PRR activation in the Arctic mouse model. In addition, the delayed expression of select AD- and DAM1-markers (specifically CD33, Tyrobp, and Trem2) in the C5aR1-deficient Arctic mice suggests a delayed switch from disease-mitigating microglia to disease-enhancing microglia in mice lacking C5aR1. These transcriptional changes resulting directly or indirectly from C5ar1 ablation coincide with the rescue of cognitive loss [18].

Inflammatory stimuli such as lipopolysaccharide or IFN-γ, or chronic inflammatory states, promote polarization of astrocytes towards a pro-inflammatory state and the subsequent expression and secretion of Lcn2 [84, 85]. Furthermore, Lcn2 promotes neuronal loss and hippocampal-dependent memory deficits in a mouse model of vascular dementia [86]. While we did not observe C5a–C5aR1-dependent changes in pan-reactive astrocyte GFAP immunoreactivity in the brain, the ArcC5a-R1KO group showed delayed expression of a subgroup of pan-reactive and A1 astrocyte genes (Lcn2, Osmr, Cd44, Vim, Serpina3n, Aqp4, C4b and C3), suggesting that while astrocytes do respond to damage associated molecular signals including those resulting from fAβ deposition, there is a delayed activation of neurotoxic astrocytes in the absence of C5aR1. It has been suggested that inflammatory microglia accentuate neurotoxic properties of astrocytes in AD contexts [19], and thus the delayed astrocyte activation seen in the absence of C5aR1 is consistent with delayed secretion of activation signals by microglia (such as TNF, but not C1q). The direct functional consequences of decreased gene expression of neurotoxic astrocyte markers, such as Lcn2, remain to be investigated. However, these findings demonstrate a complexity of astrocyte response mediators that are induced by different insults/injury and are in line with the fine tuning of immune modulating functions that the complement system exerts in multiple other challenges to the host [87–90].

Although overexpression of C5a under the GFAP promoter resulted in acceleration of behavioral deficits in the Arctic mouse, RNA-seq data revealed that overexpression of C5a in the Arctic mice delayed the rise of many inflammatory genes until later in disease progression (10 months). Interestingly, genes associated with synaptic transmission were upregulated in both C5a+ and ArcticC5a+ hippocampi. While these data appear to be opposed to the C5a-induced neuronal damage previously

Carvalho *et al. Journal of Neuroinflammation*   (2022) 19:178

Page 17 of 21

reported, the difference may be due to the in vitro cell cultures and/or the specific in vivo injury [7, 8]. Furthermore, the behavioral and transcriptional consequences of C5a overexpression in the ArcC5a+ mice suggest that in addition to C5aR1 signaling, other biochemical and cellular pathways are being induced. Indeed, C5aR2, also referred to as C5L2 or GPR77, is a second known receptor for C5a hypothesized to be a scavenger receptor for C5a and that promotes anti-inflammatory properties (reviewed in [83]). C5a binds to C5aR2 with less affinity than C5a binding to C5aR1, while the rapidly cleaved C5a fragment, C5a desArg, binds to C5aR2 with a tenfold higher affinity than to C5aR1 [91]. C5aR2 is a negative regulator of C5a–C5aR1 activity. Formation of β-arrestin–C5aR2 complex results in downregulation of C5a-induced ERK signaling and reduces LPS-induced inflammation [92]. Furthermore, C5aR2 can interact with C5aR1, promoting C5aR1 internalization via recruitment of β-arrestin and thus again downregulation of ERK signaling [83]. Genetic ablation of C5aR2 in mouse models of ischemia–reperfusion injury [93] or spinal cord injury [94] worsens recovery outcomes, while C5aR1 inhibition in these C5aR2-deficient mice eliminates the enhanced pathology due to the absence of C5aR2. C5aR2 agonism also reduces C5a–C5aR1-mediated inflammatory response to toll-like receptors, c-type lectin receptors, or cytosolic DNA sensor stimulator of IFN genes [95], all demonstrating that C5aR2 can play an important role in mitigating C5aR1-dependent inflammatory responses to injury or pathology.

We observed peak hippocampal expression of most complement pathway genes at 7–10 months in the Arc and ArcC5aR1KO mice. Surprisingly, peak complement expression in the ArcC5a+ mice was delayed to 10 months. Consistent with the findings here, others have reported that stimulation with C5a increases gene expression of C5ar1 and C3ar1 in human-derived dendritic cells [96]. Furthermore, upregulation of C3aR has been shown to induce C3 gene upregulation in human primary keratinocytes [97]. Once C3a is generated from cleaved C3, it is quickly cleaved again to form C3a-desArg. C3a can bind C3aR and C5aR2, but C3a-desArg only interacts with C5aR2 [98]. C3a-C3aR binding under pathological conditions has been shown to mitigate inflammatory cytokine and chemokine production, particularly in acute injury ([99] and reviewed in [100]). Thus, while further studies are needed to support this hypothesis, elevated levels of C5a in the ArcC5a+ mice may stimulate C3 production and cleavage at the onset of plaque pathology thereby contributing to suppression of C5a-induced neuroinflammation via indirect effects on C3aR and C5aR2 signaling. Thus, the anti-inflammatory gene expression in the presence of high concentrations of C5a, emphasizes the therapeutic advantage of the inhibition of C5aR1, without interfering with other anti-inflammatory signaling as an optimal efficacious strategy for modulating the consequences of C5a generation in AD and perhaps AD-related dementias.

C5a overexpression also induced genes involved in lipids and cholesterol metabolic processes, some of which were reduced upon C5ar1 deletion in the Arctic mouse and further enhanced (at later ages) by the transgenic expression of C5a. Although cholesterol cannot cross the blood–brain barrier, high levels of circulating cholesterol have been correlated with increased risk of dementia and drugs that reduced levels of cholesterol have been shown to reduce prevalence of AD [101, 102]. Our results suggest that cholesterol metabolism may be influenced by C5a–C5aR1 signaling and that C5aR1 inhibition may improve brain cholesterol balance.

The clusters detected in our study have a partial overlap (94 genes) with the AD subtype signatures described by [4]. Our Rc6 cluster shared 26 genes with the C1 (classic 1) subtype, characterized by increase in immune response and decreased synaptic signaling. Complement C1q genes are part of the C1 cluster. We also found shared upregulated genes related to the phagosome pathway: Itgb5, Tlr1 and Tlr2 and the astrocyte marker Gfap. In the case of lipid metabolism, the gene Lipa is found in Rc7 and it is shared with the intermediate signatures B1 (intermediate 1) and B2 (intermediate 2). Our cluster Rc3 and Rc4 (driven by overexpression of C5a) were enriched for terms related to GABAergic synapse, but when compared to the AD subtypes, Gabrb2 was downregulated in C1. Gabrb2 appears as part of 3 human AD subtype signatures: C1, A (Atypical) and C2 (Classic 2), as downregulated, upregulated and downregulated, respectively. The main differences driving our clusters compared to the signatures described by Neff et al. [4], can be explained by the fact that their signatures are a mixture of up and downregulated genes, while our clusters are based on sharing the same gene expression patterns. However, different tissue preparation, sources, and regions could be influencing the differences seen. Importantly, both human and mouse model studies agree with the upregulation of immune response genes.

Consistent with RNA-seq gene expression, immunohistochemistry showed markedly induced levels of CD11b and CD68 in all Arctic groups at 5–10 months in hippocampus and cortex. Microglia surround Aβ plaques and promote elimination of deleterious proteins [103], and thus, the early increase in CD11b high microglia in both Arc and ArcC5R1KO mice may be indicative of a microglial disease-mitigating DAM response to amyloid accumulation in the Arc model.

Carvalho *et al. Journal of Neuroinflammation*　(2022) 19:178

Page 18 of 21

CD11c was also increased in all Arctic mice compared to WT, but at 7 months, the increase was not as pronounced in the ArcC5aR1KO or ArcC5a+ hippocampi compared to Arctic. By 10 months, CD11c levels were comparable between all Arctic groups, suggesting a delay, but not a complete attenuation of differentiation/polarization of this microglial state or subset activation. CD11c+ microglia are sparse in the healthy brain, but in models of AD, their proliferation is tightly associated with plaque pathology [59, 104]. In the 5xFAD mouse model of AD, CD11c+ microglia are characterized by the elevation of disease-associated genes [105]. Transcriptional characterization of CD11c+ microglia in the APP/PS1 AD model showed that these cells express higher levels of genes associated with cell adhesion, migration, phagocytosis, and lipid/cholesterol processes [59]. In the study by Keren-Shaul et al. [105], CD11c+ microglia contain populations of DAM and homeostatic microglia in the 5xFAD model. As disease progresses, the proportion of CD11c+ DAM relative to homeostatic microglia increases, such that by the time robust neuronal loss and severe cognitive decline are observed, the majority of CD11c+ microglia are DAM, containing high expression of DAM markers Csf1 and Lpl, particularly in microglia that surround plaques [105]. Previous studies suggest that Trem2 may influence the transition of CD11c+ microglia from homeostatic to CD11c+ microglia DAM [105, 106]. Interestingly, the reduction in CD11c we observed by IHC at 7 months in the ArcC5aR1KO and ArcC5a+ hippocampus is associated with suppression of Trem2 gene expression at 7 months in these mice relative to Arc mice (Fig. 3A). Thus, it is possible that C5aR1, by synergizing with other DAM mediators such as Trem2 and/or Tyrobp, promotes the accumulation of CD11c+ microglia in plaque-filled areas to promote phagocytosis as a response to injury. However, the overload of plaques that is not reduced in the Arctic mouse model may lead to a "tipping point" where C5a–C5aR1 modulation is not protective. By immunohistochemistry, CD11c was specifically found on microglia that were in contact with amyloid plaques similar to C5aR1 expression, suggesting that these cells are responding to deposited fibrillar amyloid and may play an important role in the immune response to AD pathology [59]. Single cell RNA-seq may be able to further functionally define microglia subtypes based on C5aR1, CD11c, and other markers. Of note, since the upregulation of C5aR1 occurs largely in microglia near the plaques, with a paucity of C5aR1 staining of microglia distant from the plaques [20], blocking C5aR1 may have limited or no consequences on homeostatic microglial functions.

Conclusions

Eliminating C5aR1 from the Arctic mice delayed or reduced expression of genes enriched for inflammatory signaling pathways and microglial and astrocyte cell activation. Given the lack of altered amyloid plaque accumulation in the ArcC5aR1KO mice, these results demonstrate a separation between genes whose expression change in response to amyloid plaque deposition and genes whose expression change in response to C5a–C5aR1 signaling and thus enhanced inflammation. Ablation of C5ar1 in Arctic mice also delayed upregulation of some complement components, including C4b and C3ar1, suggesting that targeted inhibition of C5aR1 may directly or indirectly (via reduced inflammatory and neurotoxic environment) limit the supply of upstream complement components, such as C4b, thereby controlling excessive synaptic pruning as well as microglial activation. Taken together, these data are consistent with a neuroprotective effect of inhibition of the potent anaphylatoxin C5a–C5aR1 interaction, while leaving C1q and C3 immunoprotection intact, making C5a–C5aR1 signaling a promising therapeutic target for AD.

Abbreviations

AD: Alzheimer's disease; ALS: Amyotrophic lateral sclerosis; Ast: Astrocytes; Aβ: Amyloid beta; CP: Complement pathway; CPM: Count per million; DAM: Disease-associated microglia; DI: Discrimination index; FDR: False discovery rate; GO: Gene ontology; LNA: Locked nucleic acid; MAC: Membrane attack complex; Mic: Microglia; OLM: Object location memory; Rc: RNA cluster; TMM: Trimmed mean of *M*-values; TPM: Transcripts per million; TSO: Template-switching oligo.

Supplementary Information

The online version contains supplementary material available at https://doi.org/10.1186/s12974-022-02539-2.

Additional file 1: Fig S1. Presence of the C5aGFAP transgene increases C5a protein levels in brain. **Fig S2.** Locomotion and exploration during open field and object location memory training at 7 months. **Fig S3.** C5aR1 ablation reduces dystrophic neurites and reduces toxicity of amyloid plaques. **Fig S4.** Differential expression analysis show lack of sex-specific changes in gene expression in the Arctic mice. **Fig S5.** C5ar1 knockout in Arctic mice delays expression of characteristic AD and astrocyte-associated genes. **Fig S6.** Plaque accumulation is faster in hippocampus compared to cortex and is unaltered by C5a–C5aR1 modulation. **Fig S7.** Iba1 and CD68 not altered by C5a-C5aR1 modulation in Arctic mice, mirroring gene expression. **Fig S8.** Astrocyte polarization state in Arctic, ArcticC5aR1KO, and ArcticC5a+ mice.

Author contributions

KC contributed to experimental design, prepared libraries, analyzed RNA-seq data, and was a major contributor in writing the manuscript; NDS contributed to experimental design, prepared libraries, performed IHC experiments,

Carvalho *et al. Journal of Neuroinflammation*   (2022) 19:178

Page 19 of 21

Availability of data and materials
The accession number for the sequencing data reported in this paper is GEO: GSE197591.

Declarations

Ethics approval and consent to participate
The Institutional Animal Care and Use Committee of University of California at Irvine approved all animal procedures, and experiments were performed according to the NIH Guide for the Care and Use of laboratory animals.

Consent for publication
Not applicable.

Competing interests
The authors declare they have no competing interests.

Author details
[1]Department of Developmental & Cell Biology, University of California, Irvine, Irvine, CA 92697, USA. [2]Department of Molecular Biology & Biochemistry, University of California, Irvine, 3205 McGaugh Hall, Irvine, CA 92697-3900, USA. [3]Department of Neurobiology and Behavior, University of California, Irvine, Irvine, CA, USA. [4]Department of Pathology and Laboratory Medicine, University of California, Irvine, School of Medicine, Irvine, CA, USA.

References
1. DeTure MA, Dickson DW. The neuropathological diagnosis of Alzheimer's disease. Mol Neurodegener. 2019;14(1):32.
2. Heneka MT, Carson MJ, El Khoury J, Landreth GE, Brosseron F, Feinstein DL, et al. Neuroinflammation in Alzheimer's disease. Lancet Neurol. 2015;14(4):388–405.
3. Sarlus H, Heneka MT. Microglia in Alzheimer's disease. J Clin Investig. 2017;127(9):3240–9.
4. Neff RA, Wang M, Vatansever S, Guo L, Ming C, Wang Q, et al. Molecular subtyping of Alzheimer's disease using RNA sequencing data reveals novel mechanisms and targets. Sci Adv. 2021;7(2):eabb5398.
5. Schartz ND, Tenner AJ. The good, the bad, and the opportunities of the complement system in neurodegenerative disease. J Neuroinflamm. 2020;17(1):354.
6. Tenner AJ. Complement-mediated events in Alzheimer's disease: mechanisms and potential therapeutic targets. J Immunol. 2020;204(2):306–15.
7. Pavlovski D, Thundyil J, Monk PN, Wetsel RA, Taylor SM, Woodruff TM. Generation of complement component C5a by ischemic neurons promotes neuronal apoptosis. FASEB J. 2012;26(9):3680–90.
8. Hernandez MX, Namiranian P, Nguyen E, Fonseca MI, Tenner AJ. C5a increases the injury to primary neurons elicited by fibrillar amyloid beta. ASN Neuro. 2017;9(1):1759091416687871.
9. Fonseca MI, Ager RR, Chu SH, Yazan O, Sanderson SD, LaFerla FM, et al. Treatment with a C5aR antagonist decreases pathology and enhances behavioral performance in murine models of Alzheimer's disease. J Immunol. 2009;183(2):1375–83.
10. Woodruff TM, Costantini KJ, Crane JW, Atkin JD, Monk PN, Taylor SM, et al. The complement factor C5a contributes to pathology in a rat model of amyotrophic lateral sclerosis. J Immunol. 2008;181(12):8727–34.
11. Wang HA, Lee JD, Lee KM, Woodruff TM, Noakes PG. Complement C5a–C5aR1 signalling drives skeletal muscle macrophage recruitment in the hSOD1G93A mouse model of amyotrophic lateral sclerosis. Skelet Muscle. 2017;7(1):10.
12. Buckingham SC, Ramos TN, Barnum SR. Complement C5-deficient mice are protected from seizures in experimental cerebral malaria. Epilepsia. 2014;55(12):e139–42.
13. Benson MJ, Thomas NK, Talwar S, Hodson MP, Lynch JW, Woodruff TM, et al. A novel anticonvulsant mechanism via inhibition of complement receptor C5ar1 in murine epilepsy models. Neurobiol Dis. 2015;76:87–97.
14. Li L, Xiong Z-Y, Qian ZM, Zhao T-Z, Feng H, Hu S, et al. Complement C5a is detrimental to histological and functional locomotor recovery after spinal cord injury in mice. Neurobiol Dis. 2014;66:74–82.
15. Ennis D, Yeung RS, Pagnoux C. Long-term use and remission of granulomatosis with polyangiitis with the oral C5a receptor inhibitor avacopan. BMJ Case Rep. 2020;13(10):e236236.
16. Tesar V, Hruskova Z. Avacopan in the treatment of ANCA-associated vasculitis. Expert Opin Investig Drugs. 2018;27(5):491–6.
17. Vergunst CE, Gerlag DM, Dinant H, Schulz L, Vinkenoog M, Smeets TJ, et al. Blocking the receptor for C5a in patients with rheumatoid arthritis does not reduce synovial inflammation. Rheumatology (Oxford). 2007;46(12):1773–8.
18. Hernandez MX, Jiang S, Cole TA, Chu S-H, Fonseca MI, Fang MJ, et al. Prevention of C5aR1 signaling delays microglial inflammatory polarization, favors clearance pathways and suppresses cognitive loss. Mol Neurodegener. 2017;12(1):66.
19. Liddelow SA, Guttenplan KA, Clarke LE, Bennett FC, Bohlen CJ, Schirmer L, et al. Neurotoxic reactive astrocytes are induced by activated microglia. Nature. 2017;541:481.
20. Ager RR, Fonseca MI, Chu SH, Sanderson SD, Taylor SM, Woodruff TM, et al. Microglial C5aR (CD88) expression correlates with amyloid-beta deposition in murine models of Alzheimer's disease. J Neurochem. 2010;113(2):389–401.
21. Vogel-Ciernia A, Wood MA. Examining object location and object recognition memory in mice. Curr Protoc Neurosci. 2014;69:8.31.1-17.
22. Cheng IH, Palop JJ, Esposito LA, Bien-Ly N, Yan F, Mucke L. Aggressive amyloidosis in mice expressing human amyloid peptides with the Arctic mutation. Nat Med. 2004;10(11):1190–2.
23. Reiman R, Campos Torres A, Martin BK, Ting JP, Campbell IL, Barnum SR. Expression of C5a in the brain does not exacerbate experimental autoimmune encephalomyelitis. Neurosci Lett. 2005;390(3):134–8.
24. Hollmann TJ, Mueller-Ortiz SL, Braun MC, Wetsel RA. Disruption of the C5a receptor gene increases resistance to acute Gram-negative bacteremia and endotoxic shock: opposing roles of C3a and C5a. Mol Immunol. 2008;45(7):1907–15.
25. Taketo M, Schroeder AC, Mobraaten LE, Gunning KB, Hanten G, Fox RR, et al. FVB/N: an inbred mouse strain preferable for transgenic analyses. Proc Natl Acad Sci USA. 1991;88(6):2065–9.
26. Picelli S, Faridani OR, Björklund AK, Winberg G, Sagasser S, Sandberg R. Full-length RNA-seq from single cells using Smart-seq2. Nat Protoc. 2014;9(1):171–81.
27. Dobin A, Davis CA, Schlesinger F, Drenkow J, Zaleski C, Jha S, et al. STAR: ultrafast universal RNA-seq aligner. Bioinformatics. 2013;29(1):15–21.
28. Li B, Dewey CN. RSEM: accurate transcript quantification from RNA-Seq data with or without a reference genome. BMC Bioinform. 2011;12:323.
29. Zhang Y, Parmigiani G, Johnson WE. ComBat-seq: batch effect adjustment for RNA-seq count data. NAR Genom Bioinform. 2020;2(3):lqaa078.
30. Robinson MD, McCarthy DJ, Smyth GK. edgeR: a Bioconductor package for differential expression analysis of digital gene expression data. Bioinformatics. 2010;26(1):139–40.

Carvalho *et al. Journal of Neuroinflammation*   (2022) 19:178

Page 20 of 21

31. Mukaka MM. Statistics corner: a guide to appropriate use of correlation coefficient in medical research. Malawi Med J. 2012;24(3):69–71.

32. Nueda MJ, Tarazona S, Conesa A. Next maSigPro: updating maSigPro bioconductor package for RNA-seq time series. Bioinformatics. 2014;30(18):2598–602.

33. Huang DW, Sherman BT, Tan Q, Collins JR, Alvord WG, Roayaei J, et al. The DAVID Gene Functional Classification Tool: a novel biological module-centric algorithm to functionally analyze large gene lists. Genome Biol. 2007;8(9):R183.

34. Zhou Y, Zhou B, Pache L, Chang M, Khodabakhshi AH, Tanaseichuk O, et al. Metascape provides a biologist-oriented resource for the analysis of systems-level datasets. Nat Commun. 2019;10(1):1523.

35. Armoskus C, Mota T, Moreira D, Tsai HW. Effects of prenatal testosterone exposure on sexually dimorphic gene expression in the neonatal mouse cortex and hippocampus. J Steroids Horm Sci. 2014;5(3):1000139.

36. Forner S, Kawauchi S, Balderrama-Gutierrez G, Kramár EA, Matheos DP, Phan J, et al. Systematic phenotyping and characterization of the 5xFAD mouse model of Alzheimer's disease. bioRxiv. 2021:2021.02.17.431716.

37. Klos A, Wende E, Wareham KJ, Monk PN. International Union of Basic and Clinical Pharmacology. [corrected]. LXXXVII. Complement peptide C5a, C4a, and C3a receptors. Pharmacol Rev. 2013;65(1):500–43.

38. Lee JD, Coulthard LG, Woodruff TM. Complement dysregulation in the central nervous system during development and disease. Semin Immunol. 2019;45:101340.

39. Chen G, Tan CS, Teh BK, Lu J. Molecular mechanisms for synchronized transcription of three complement C1q subunit genes in dendritic cells and macrophages. J Biol Chem. 2011;286(40):34941–50.

40. Lattin JE, Greenwood KP, Daly NL, Kelly G, Zidar DA, Clark RJ, et al. Beta-arrestin 2 is required for complement C1q expression in macrophages and constrains factor-independent survival. Mol Immunol. 2009;47(2–3):340–7.

41. Verheijen J, Sleegers K. Understanding Alzheimer disease at the interface between genetics and transcriptomics. Trends Genet. 2018;34(6):434–47.

42. Tanzi RE. The genetics of Alzheimer disease. Cold Spring Harb Perspect Med. 2012;2(10):a006296.

43. Bertram L, Tanzi RE. Alzheimer disease risk genes: 29 and counting. Nat Rev Neurol. 2019;15(4):191–2.

44. Efthymiou AG, Goate AM. Late onset Alzheimer's disease genetics implicates microglial pathways in disease risk. Mol Neurodegener. 2017;12(1):43.

45. Tsai AP, Lin PB, Dong C, Moutinho M, Casali BT, Liu Y, et al. INPP5D expression is associated with risk for Alzheimer's disease and induced by plaque-associated microglia. Neurobiol Dis. 2021;153: 105303.

46. Yoshino Y, Yamazaki K, Ozaki Y, Sao T, Yoshida T, Mori T, et al. INPP5D mRNA expression and cognitive decline in Japanese Alzheimer's disease subjects. J Alzheimers Dis. 2017;58(3):687–94.

47. Cristóvão JS, Gomes CM. S100 proteins in Alzheimer's disease. Front Neurosci. 2019;13:463.

48. Choi M, Kim H, Yang E-J, Kim H-S. Inhibition of STAT3 phosphorylation attenuates impairments in learning and memory in 5XFAD mice, an animal model of Alzheimer's disease. J Pharmacol Sci. 2020;143(4):290–9.

49. Habib N, McCabe C, Medina S, Varshavsky M, Kitsberg D, Dvir-Szternfeld R, et al. Disease-associated astrocytes in Alzheimer's disease and aging. Nat Neurosci. 2020;23(6):701–6.

50. Jha MK, Jo M, Kim JH, Suk K. Microglia-astrocyte crosstalk: an intimate molecular conversation. Neuroscientist. 2019;25(3):227–40.

51. Moynagh PN. The interleukin-1 signalling pathway in astrocytes: a key contributor to inflammation in the brain. J Anat. 2005;207(3):265–9.

52. Coulthard LG, Hawksworth OA, Li R, Balachandran A, Lee JD, Sepehrband F, et al. Complement C5aR1 signaling promotes polarization and proliferation of embryonic neural progenitor cells through PKCζ. J Neurosci. 2017;37(22):5395–407.

53. Sanchez-Mejias E, Nunez-Diaz C, Sanchez-Varo R, Gomez-Arboledas A, Garcia-Leon JA, Fernandez-Valenzuela JJ, et al. Distinct disease-sensitive GABAergic neurons in the perirhinal cortex of Alzheimer's mice and patients. Brain Pathol. 2020;30(2):345–63.

54. Sun B, Halabisky B, Zhou Y, Palop JJ, Yu G, Mucke L, et al. Imbalance between GABAergic and glutamatergic transmission impairs adult

55. neurogenesis in an animal model of Alzheimer's disease. Cell Stem Cell. 2009;5(6):624–33.

55. Mathys H, Davila-Velderrain J, Peng Z, Gao F, Mohammadi S, Young JZ, et al. Single-cell transcriptomic analysis of Alzheimer's disease. Nature. 2019;570(7761):332–7.

56. Czirr E, Castello NA, Mosher KI, Castellano JM, Hinkson IV, Lucin KM, et al. Microglial complement receptor 3 regulates brain Aβ levels through secreted proteolytic activity. J Exp Med. 2017;214(4):1081–92.

57. Linnartz B, Neumann H. Microglial activatory (immunoreceptor tyrosine-based activation motif)- and inhibitory (immunoreceptor tyrosine-based inhibition motif)-signaling receptors for recognition of the neuronal glycocalyx. Glia. 2013;61(1):37–46.

58. Haure-Mirande JV, Audrain M, Fanutza T, Kim SH, Klein WL, Glabe C, et al. Deficiency of TYROBP, an adapter protein for TREM2 and CR3 receptors, is neuroprotective in a mouse model of early Alzheimer's pathology. Acta Neuropathol. 2017;134(5):769–88.

59. Kamphuis W, Kooijman L, Schetters S, Orre M, Hol EM. Transcriptional profiling of CD11c-positive microglia accumulating around amyloid plaques in a mouse model for Alzheimer's disease. Biochim Biophys Acta. 2016;1862(10):1847–60.

60. Das S, Li Z, Noori A, Hyman BT, Serrano-Pozo A. Meta-analysis of mouse transcriptomic studies supports a context-dependent astrocyte reaction in acute CNS injury versus neurodegeneration. J Neuroinflamm. 2020;17(1):227.

61. Cribbs DH, Berchtold NC, Perreau V, Coleman PD, Rogers J, Tenner AJ, et al. Extensive innate immune gene activation accompanies brain aging, increasing vulnerability to cognitive decline and neurodegeneration: a microarray study. J Neuroinflamm. 2012;9(1):179.

62. Zhang B, Gaiteri C, Bodea LG, Wang Z, McElwee J, Podtelezhnikov AA, et al. Integrated systems approach identifies genetic nodes and networks in late-onset Alzheimer's disease. Cell. 2013;153(3):707–20.

63. Chen WT, Lu A, Craessaerts K, Pavie B, Sala Frigerio C, Corthout N, et al. Spatial transcriptomics and in situ sequencing to study Alzheimer's disease. Cell. 2020;182(4):976-91.e19.

64. Merkel PA, Niles J, Jimenez R, Spiera RF, Rovin BH, Bomback A, et al. Adjunctive treatment with avacopan, an oral C5a receptor inhibitor, in patients with antineutrophil cytoplasmic antibody-associated vasculitis. ACR Open Rheumatol. 2020;2(11):662–71.

65. Hillmen P, Muus P, Roth A, Elebute MO, Risitano AM, Schrezenmeier H, et al. Long-term safety and efficacy of sustained eculizumab treatment in patients with paroxysmal nocturnal haemoglobinuria. Br J Haematol. 2013;162(1):62–73.

66. Tenner AJ, Stevens B, Woodruff TM. New tricks for an ancient system: physiological and pathological roles of complement in the CNS. Mol Immunol. 2018;102:3–13.

67. Stephan AH, Barres BA, Stevens B. The complement system: an unexpected role in synaptic pruning during development and disease. Annu Rev Neurosci. 2012;35:369–89.

68. Stevens B, Allen NJ, Vazquez LE, Howell GR, Christopherson KS, Nouri N, et al. The classical complement cascade mediates CNS synapse elimination. Cell. 2007;131(6):1164–78.

69. Fonseca MI, Zhou J, Botto M, Tenner AJ. Absence of C1q leads to less neuropathology in transgenic mouse models of Alzheimer's disease. J Neurosci. 2004;24(29):6457–65.

70. Hong S, Beja-Glasser VF, Nfonoyim BM, Frouin A, Li S, Ramakrishnan S, et al. Complement and microglia mediate early synapse loss in Alzheimer mouse models. Science. 2016;352(6286):712–6.

71. Werneburg S, Jung J, Kunjamma RB, Ha S-K, Luciano NJ, Willis CM, et al. Targeted complement inhibition at synapses prevents microglial synaptic engulfment and synapse loss in demyelinating disease. Immunity. 2020;52(1):167-82.e7.

72. Schafer DP, Lehrman EK, Kautzman AG, Koyama R, Mardinly AR, Yamasaki R, et al. Microglia sculpt postnatal neural circuits in an activity and complement-dependent manner. Neuron. 2012;74(4):691–705.

73. Shi Q, Colodner KJ, Matousek SB, Merry K, Hong S, Kenison JE, et al. Complement C3-deficient mice fail to display age-related hippocampal decline. J Neurosci. 2015;35(38):13029–42.

74. Shi Q, Chowdhury S, Ma R, Le KX, Hong S, Caldarone BJ, et al. Complement C3 deficiency protects against neurodegeneration in aged plaque-rich APP/PS1 mice. Sci Transl Med. 2017;9(392):eaaf6295.

Carvalho *et al. Journal of Neuroinflammation*   (2022) 19:178

Page 21 of 21

75. Gomez-Arboledas A, Acharya MM, Tenner AJ. The role of complement in synaptic pruning and neurodegeneration. Immunotargets Ther. 2021;10:373–86.

76. Fraser DA, Pisalyaput K, Tenner AJ. C1q enhances microglial clearance of apoptotic neurons and neuronal blebs, and modulates subsequent inflammatory cytokine production. J Neurochem. 2010;112(3):733–43.

77. Landlinger C, Oberleitner L, Gruber P, Noiges B, Yatsyk K, Santic R, et al. Active immunization against complement factor C5a: a new therapeutic approach for Alzheimer's disease. J Neuroinflamm. 2015;12:150.

78. Cheng IH, Scearce-Levie K, Legleiter J, Palop JJ, Gerstein H, Bien-Ly N, et al. Accelerating amyloid-beta fibrillization reduces oligomer levels and functional deficits in Alzheimer disease mouse models. J Biol Chem. 2007;282(33):23818–28.

79. Hagmeyer S, Romão MA, Cristóvão JS, Vilella A, Zoli M, Gomes CM, et al. Distribution and relative abundance of S100 proteins in the brain of the APP23 Alzheimer's disease model mice. Front Neurosci. 2019;13:640.

80. Reichenbach N, Delekate A, Plescher M, Schmitt F, Krauss S, Blank N, et al. Inhibition of Stat3-mediated astrogliosis ameliorates pathology in an Alzheimer's disease model. EMBO Mol Med. 2019;11(2):e9665.

81. Petrisko TJ, Gomez-Arboledas A, Tenner AJ. Chapter Three—Complement as a powerful "influencer" in the brain during development, adulthood and neurological disorders. In: Alt FW, Murphy KM, editors. Advances in immunology, vol. 152. Cambridge: Academic Press; 2021. p. 157–222.

82. Reis ES, Mastellos DC, Hajishengallis G, Lambris JD. New insights into the immune functions of complement. Nat Rev Immunol. 2019;19(8):503–16.

83. Li XX, Lee JD, Kemper C, Woodruff TM. The complement receptor C5aR2: a powerful modulator of innate and adaptive immunity. J Immunol. 2019;202(12):3339–48.

84. Jang E, Kim JH, Lee S, Kim JH, Seo JW, Jin M, et al. Phenotypic polarization of activated astrocytes: the critical role of lipocalin-2 in the classical inflammatory activation of astrocytes. J Immunol. 2013;191(10):5204–19.

85. Kim BW, Jeong KH, Kim JH, Jin M, Kim JH, Lee MG, et al. Pathogenic upregulation of glial lipocalin-2 in the Parkinsonian dopaminergic system. J Neurosci. 2016;36(20):5608–22.

86. Kim JH, Ko PW, Lee HW, Jeong JY, Lee MG, Kim JH, et al. Astrocyte-derived lipocalin-2 mediates hippocampal damage and cognitive deficits in experimental models of vascular dementia. Glia. 2017;65(9):1471–90.

87. Clarke EV, Tenner AJ. Complement modulation of T cell immune responses during homeostasis and disease. J Leukoc Biol. 2014;96(5):745–56.

88. Merle NS, Singh P, Rahman J, Kemper C. Integrins meet complement: the evolutionary tip of an iceberg orchestrating metabolism and immunity. Br J Pharmacol. 2020;178:2754–70.

89. Lo MW, Woodruff TM. Complement: bridging the innate and adaptive immune systems in sterile inflammation. J Leukoc Biol. 2020;108(1):339–51.

90. Hess C, Kemper C. Complement-mediated regulation of metabolism and basic cellular processes. Immunity. 2016;45(2):240–54.

91. Cain SA, Monk PN. The orphan receptor C5L2 has high affinity binding sites for complement fragments C5a and C5a des-Arg(74). J Biol Chem. 2002;277(9):7165–9.

92. Croker DE, Monk PN, Halai R, Kaeslin G, Schofield Z, Wu MC, et al. Discovery of functionally selective C5aR2 ligands: novel modulators of C5a signalling. Immunol Cell Biol. 2016;94(8):787–95.

93. Wu MCL, Lee JD, Ruitenberg MJ, Woodruff TM. Absence of the C5a receptor C5aR2 worsens ischemic tissue injury by increasing C5aR1-mediated neutrophil infiltration. J Immunol. 2020;205(10):2834–9.

94. Biggins PJC, Brennan FH, Taylor SM, Woodruff TM, Ruitenberg MJ. The alternative receptor for complement component 5a, C5aR2, conveys neuroprotection in traumatic spinal cord injury. J Neurotrauma. 2017;34(12):2075–85.

95. Li XX, Clark RJ, Woodruff TM. C5aR2 activation broadly modulates the signaling and function of primary human macrophages. J Immunol. 2020;205(4):1102–12.

96. Li K, Fazekasova H, Wang N, Peng Q, Sacks SH, Lombardi G, et al. Functional modulation of human monocytes derived DCs by anaphylatoxins C3a and C5a. Immunobiology. 2012;217(1):65–73.

97. Purwar R, Wittmann M, Zwirner J, Oppermann M, Kracht M, Dittrich-Breiholz O, et al. Induction of C3 and CCL2 by C3a in keratinocytes: a novel autocrine amplification loop of inflammatory skin reactions. J Immunol. 2006;177(7):4444–50.

98. Kalant D, Cain SA, Maslowska M, Sniderman AD, Cianflone K, Monk PN. The chemoattractant receptor-like protein C5L2 binds the C3a des-Arg^{77}/Acylation-stimulating Protein *. J Biol Chem. 2003;278(13):11123–9.

99. Wei L-L, Ma N, Wu K-Y, Wang J-X, Diao T-Y, Zhao S-J, et al. Protective role of C3aR (C3a Anaphylatoxin Receptor) against atherosclerosis in atherosclerosis-prone mice. Arterioscler Thromb Vasc Biol. 2020;40(9):2070–83.

100. Coulthard LG, Woodruff TM. Is the complement activation product C3a a proinflammatory molecule? Re-evaluating the evidence and the myth. J Immunol. 2015;194(8):3542–8.

101. Loera-Valencia R, Goikolea J, Parrado-Fernandez C, Merino-Serrais P, Maioli S. Alterations in cholesterol metabolism as a risk factor for developing Alzheimer's disease: potential novel targets for treatment. J Steroid Biochem Mol Biol. 2019;190:104–14.

102. Varma VR, Busra Luleci H, Oommen AM, Varma S, Blackshear CT, Griswold ME, et al. Abnormal brain cholesterol homeostasis in Alzheimer's disease-a targeted metabolomic and transcriptomic study. NPJ Aging Mech Dis. 2021;7(1):11.

103. Hickman S, Izzy S, Sen P, Morsett L, El Khoury J. Microglia in neurodegeneration. Nat Neurosci. 2018;21(10):1359–69.

104. Wu X, Saito T, Saido TC, Barron AM, Ruedl C. Microglia and CD206(+) border-associated mouse macrophages maintain their embryonic origin during Alzheimer's disease. Elife. 2021;10:e71879.

105. Keren-Shaul H, Spinrad A, Weiner A, Matcovitch-Natan O, Dvir-Sztern-feld R, Ulland TK, et al. A unique microglia type associated with restricting development of Alzheimer's disease. Cell. 2017;169(7):1276-90.e17.

106. Sayed FA, Kodama L, Fan L, Carling GK, Udeochu JC, Le D, et al. AD-linked R47H-TREM2 mutation induces disease-enhancing microglial states via AKT hyperactivation. Sci Transl Med. 2021;13(622):eabe3947.

Publisher's Note